ADAPTIVE EXCITATION CONTROL IN POWER SYSTEMS

A Thesis

by

PEI-CHEN CHIU

Submitted to the Office of Graduate Studies of
Texas A&M University
in partial fulfillment of the requirements for the degree of

MASTER OF SCIENCE

May 2006

Major Subject: Electrical Engineering

ADAPTIVE EXCITATION CONTROL IN POWER SYSTEMS

A Thesis

by

PEI-CHEN CHIU

Submitted to the Office of Graduate Studies of
Texas A&M University
in partial fulfillment of the requirements for the degree of

MASTER OF SCIENCE

Approved by:

Chair of Committee, Garng Huang
Committee Members, Aniruddha Datta
Prasad Enjeti
Joseph E. Pasciak
Head of Department, Costas Georghiades

May 2006

Major Subject: Electrical Engineering

ABSTRACT

Adaptive Excitation Control in Power Systems.

(May 2006)

Pei-Chen Chiu, B.S., National Chiao Tung University

Chair of Advisory Committee: Dr. Garng Huang

This thesis presents an adaptive excitation controller of power systems. The control law is derived by using *model reference adaptive control* (MRAC) or *adaptive pole placement control* (APPC) and an equilibrium tracking mechanism is implemented to obtain equilibrium. By our approaches, system damping improvement is achieved to increase loadability as well as strengthen stability properties.

To my mother

ACKNOWLEDGEMENTS

I would like to thank my committee chair, Dr. Huang, and my committee members, Dr. Datta, Dr. Enjeti, and Dr. Pasciak for their guidance and support throughout my course of research.

TABLE OF CONTENTS

Page

CHAPTER Page

LIST OF FIGURES

FIGURE Page

FIGURE Page

FIGURE Page

CHAPTER I

INTRODUCTION

In last decades, the power systems are being operated under increasing stressed conditions due to transmission expansion, increased electricity consumption, new loading patterns for deregulation of power market, and etc. Under these stressed conditions, slow voltage drop or even voltage collapse have become a serious operating concern and therefore dynamic analysis and control design of power system for voltage stability issues has been more critical [1][2][3].

The excitation control of power generator is one of the most effective and economical techniques for improve dynamic voltage performance and voltage stability of power systems. It has been approached by classic control and linear modern control techniques with good results, but only locally valid. Due to the nonlinearilities of various components of power systems and the inherent characteristics of changing load, the operating points of power system may change during a daily cycle. As a result, a fixed controller that is optimal under one operating condition may become unsuitable for another operating condition.

In view of this, engineers have applied the diverse control laws to make controller adapt to plant parameter changes. In the recent decades, various control techniques have been proposed for dealing with large parameter variations.

The thesis follows the style and format of *IEEE Transactions on Automatic Control.*

For example, variable structure controls had been applied to power systems by some authors [4][5]. Feedback linearization techniques were proposed to design controls to e-nlarge stable region [6][7]. Nonlinear adaptive controls are also proposed [8].

This thesis presents an adaptive excitation controller of power systems. The control law is derived by using *model reference adaptive control* (MRAC) and *adaptive pole placement control* (APPC) [9][10]. An equilibrium tracking mechanism is implemented to obtain equilibrium value and the adaptive control is applied to stabilize the equilibrium. By our approaches, system damping improvement is achieved to increase loadability as well as strengthen stability properties. Besides, since our adaptive control can accommodate uncertainty parameters (in the thesis, we consider the uncertain load), the system will be robust in practical application. The implementation of our control can be achieved by the digital excitation without too much cost [11]. Finally, power systems examples are demonstrated our approaches and applications.

1.1 Modeling of Power Systems

The dynamics of a large class of physic systems are commonly expressed in a parameter dependent differential- algebraic equation (DAE) form [1][2]:

$$\dot{x} = f(x, y, p) \quad f : \Re^{n+m+q} \to \Re^{n} \tag{1.1}$$

$$0 = g(x, y, p) \quad g : \Re^{n+m+q} \to \Re^{m} \tag{1.2}$$

$$x \in X \subset \Re^{n},\ y \in Y \subset \Re^{m},\ p \in P \subset \Re^{q}$$

In the state-space X x Y , dynamic state variables x and instantaneous state variables y are distinguished. The differential equation (1.1) represents the dynamic

behavior while the algebraic equation (1.2) represents algebraic constraints. Parameters p define specific system configurations and the operation condition.

For power systems, typical dynamic state variables are the time-dependent values of generator voltages and rotor phases and speed; instantaneous variables are bus voltage and other load flow variables. The parameters p are lines, buses, equipment coefficients, set-points, load and etc. The dynamics of the generators, control devices and the load dynamics together define the f equations. The constraints g are defined by the power flow equations of the transmission system.

1.2 Power System Dynamics Stability

We usually analyze nonlinear system dynamics through observing time responses and eigenvalue solutions. For a given parameter p, the linearized dynamic expression of DAE is as below [2][12][13]:

$$\begin{bmatrix} \Delta \dot{x} \\ 0 \end{bmatrix} = J_u \begin{bmatrix} \Delta x \\ \Delta y \end{bmatrix} \tag{1.3}$$

$$J_u = \begin{bmatrix} f_x & f_y \\ g_x & g_y \end{bmatrix} \tag{1.4}$$

When g_y is nonsingular, the algebraic variable Δy can be eliminate from (1.3) and get a reduced ODE (ordinary-differential equation) as (1.5),

$$\Delta \dot{x} = J_r \Delta x \tag{1.5}$$

$$J_r = [f_x - f_y g_y^{-1} g_x] \tag{1.6}$$

J_r is called the reduced Jacobian matrix (RJM). The stability of an equilibrium point of the DAE for the given parameter p depends on the eigenvalues of matrix J_r. J_r could be also referred to as a function of the parameter p. As the system goes through different operating conditions, the parameter p change leads to different value for J_r. For the power systems with the constant controllers, J_r may be a stable matrix for some parameter p while unstable for another p. Our goal of the thesis is design an auxiliary adaptive feedback controller to stabilize J_r for changing or uncertain parameter p.

Let's assume that the system parameter p is uncertain or changing but its equilibrium value for the corresponding p is known (the assumption will be released by our equilibrium tracking mechanism at last) and rewrite equation (1.5) with input u_p and output y_p

$$\begin{aligned} \Delta \dot{x} &= A_i \Delta x + B_i \Delta u_p \\ \Delta y_p &= C_i \Delta x \end{aligned} \tag{1.7}$$

A_i, B_i, C_i is depend on the system parameter p. We can refer to the original nonlinear DAE system (1.1)-(1.2) as a linear system (1.7) with uncertain parameter A_i, B_i, C_i around a small enough neighborhood of the equilibrium and thus we could apply some linear adaptive laws to control the linear system with uncertain parameter A_i, B_i, C_i.

Because the output Δy_p of the system carries information about states Δx as well as the parameters, one may design a sophisticated feedback controller which is able to learn about the parameters A_i, B_i, C_i changes by processing the output and use the appropriate

controller gains to accommodate and stabilize the system. The way of changing the controller gains in response to changes of the system led to the base of adaptive controls.

In the thesis, the power load is referred as a changing or uncertain parameter. We would propose a dynamic mechanism to track equilibrium value as the load p changes (when the system has the equilibrium). After obtaining the value of equilibrium, we could observe the dynamic behavior around the equilibrium and apply several adaptive control laws for the linear system with uncertain parameter eq. (1.7) such that the output Δy_p trace and follow the bounded reference signal y_m. The adaptive control makes the local dynamic stability along the original PV curve and therefore increases loadability.

Since our approaches can deal with the uncertain load, it will be able to accommodate parameter uncertainty and thus more robust. It should be noticed, however, that our approach is derived according linearized model of eq. (1.7) around the equilibrium and therefore is only valid for a small enough neighborhood of the equilibrium.

In the following section 1.3, we briefly introduce two popular linear adaptive control schemes to deal with the plant with unknown parameters: model reference control and adaptive pole placement control.

1.3 Model Reference Adaptive Control and Adaptive Pole Placement Control

Model reference adaptive control (MRAC) is derived from the model reference control (MRC). In MRC, its objective is to find the feedback control law that changes the structure and dynamics of the system so that its I/O properties are exactly the same

as those of the reference model. The structure of MRC scheme for a LTI, SISO system is shown in Fig. 1.1. The transfer function $W_m(s)$ of the reference model is design so that for a given reference input $r(t)$ the output $y_m(t)$ represents the desired response the plant output $y(t)$ should follow. The feedback controller denoted by $C(\theta_c^*)$ is designed so that all signals are bounded and the closed –loop transfer function from r to y is equal to $W_m(s)$ .The design of $C(\theta_c^*)$ requires the knowledge of the coefficients of $G(s) = G(s, \theta^*)$ and θ_c^* may be computed by solving an algebraic equation of the form

$$\theta_c^* = F(\theta^*) \tag{1.8}$$

It should be noticed that the plant model has to be minimum phase, i.e. with no unstable zeros, because the cancellation of the unstable zero may lead to unbounded signals [9][10].

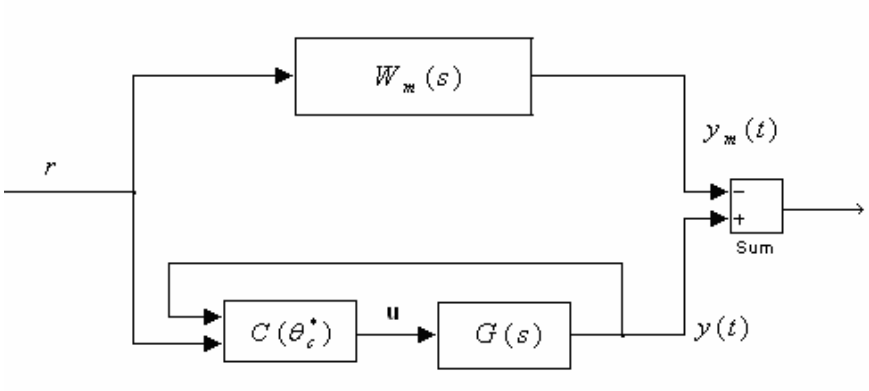

Fig. 1.1 Model Reference Control

When θ^* is unknown the MRC scheme cannot be implemented because θ_c^* cannot be calculated by (1.8). One way of dealing with the unknown parameter case is to use the certainty equivalence approach to replace the unknown θ_c^* with its estimate $\theta_c(t)$ obtained by using adaptive approaches. Fig.1.2 shows a typical MRAC diagram.

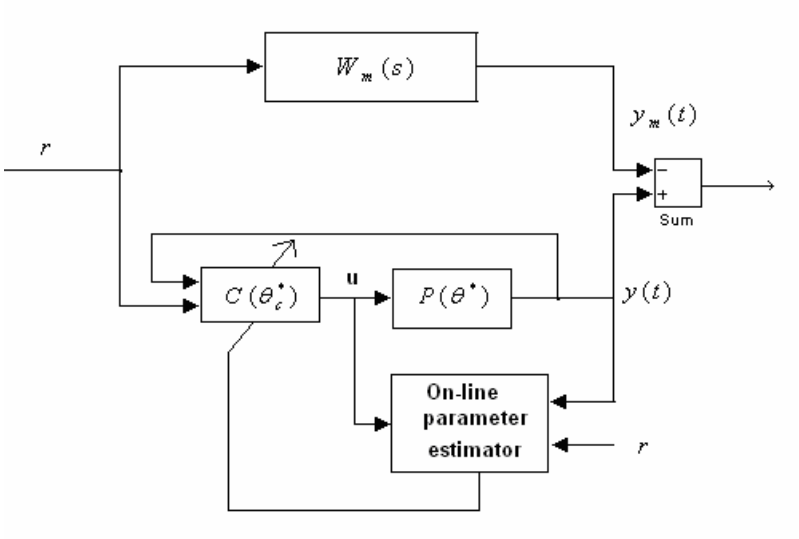

Fig. 1.2 Model Reference Adaptive Control

Another popular control schemes are referred as pole placement control (PPC). It can translate the locations of the poles of the plant into the desired locations of the poles of the closed-loop plant. These schemes do not involve zero-pole cancellation and therefore

are applicable to both minimum and non-minimum phase plants. The combination of a pole placement control law with a parameter estimator or an adaptive control law leads to an adaptive pole placement (APPC) that is often referred as self-tuning regulators in the literature of adaptive controls and can be used to control the systems with unknown parameters.

1.4 Objectives and Organization

In the thesis, we propose an adaptive controller for the power system to adapt a large range change of operation condition or uncertainly system parameters. The first step, we start with a DAE model of Eq. (1.1)(1.2). Here, we have an original DAE system with a feedback control input Δu_p represented as:

$$\begin{aligned} \dot{x} &= f(x, y, p, \Delta u_p) \\ 0 &= g(x, y, p, \Delta u_p) \end{aligned} \tag{1.9}$$

By proposing an equilibrium tracking, we track the equilibrium x_e, y_e for its corresponding p satisfying

$$\begin{aligned} 0 &= f(x_e, y_e, p, \Delta u_p = 0) \\ 0 &= g(x_e, y_e, p, \Delta u_p = 0) \end{aligned} \tag{1.10}$$

Therefore, the linear model around the equilibrium (x_e, y_e) is

$$\Delta \dot{x} = A_i \Delta x + B_i \Delta u_p \tag{1.11}$$

where

$$\Delta x = x - x_e \tag{1.12}$$

Without a feedback controller ($\Delta u_p \equiv 0$), the dynamic stability of the equilibrium x_e, y_e depends only on A_i which may be a stable or unstable matrix for the different load *p*. Therefore, we would propose some feedback adaptive control laws to resolve stability problem for the closed-loop system (1.13),

$$\Delta \dot{x} = A_i \Delta x + B_i \Delta u_p(\Delta x, \theta_c) \tag{1.13}$$

where θ_c is the control parameter. As we mentioned in the section 1.3, similarly, θ_c requires the knowledge of system parameters A_i, B_i. However, uncertain parameter p makes unknown A_i, B_i. Therefore, we need to adopt the adaptive control to obtain A_i, B_i.

The adaptive control law is usually based on two different approaches. The first approaches, referred to as a direct adaptive control, the controller parameters θ_c are estimated directly from the state Δx or the plant output Δy_p without intermediate calculations involving the plant parameter estimator for A_i, B_i. The second approaches, referred to as an indirect adaptive control, the plant parameters A_i, B_i are estimated on-line and used to calculate the controller parameters.

The direct adaptive control can be represented as,

$$\Delta u_p = h(\Delta x, \theta_c) \tag{1.14}$$

The controller parameters θ_c are direct estimated by a dynamic mechanism

$$\dot{\theta}_c = \gamma(\theta_c, \Delta x) \tag{1.15}$$

As to the indirect adaptive control, it can be represented as,

$$\Delta u_p = h(\Delta x, \theta_c) \tag{1.16}$$

The controller parameters θ_c are calculate by resolving an algebraic equation

$$\theta_c = F(\theta_p) \tag{1.17}$$

where θ_p is an estimate of plant parameter A_i, B_i, generated by an dynamic on-line estimator,

$$\dot{\theta}_p = \gamma(\theta_p, \Delta x) \tag{1.18}$$

It should be noticed that in the practical applications, not all of the states Δx are measurable but only output Δy_p is available for measurement. In such cases, Δx is replaced by Δy_p in equations (1.14)-(1.18) and referred to as output feedback control.

The implementation of the above adaptive controller must be generated by Δx and therefore requires the knowledge of the equilibrium value x_e of equation (1.10), which would vary as operating condition p_i changes and is not available. We resolve this situation by implementing a dynamic tracking of the equilibrium position. It could be achieved by thinking of the equilibrium as an uncertainty parameter in control law and applying a certainty equivalence adaptive law. That is, instead of using the true value x_e, we use an estimate $\hat{x}_e$ with its dynamic mechanism described by

$$\dot{\hat{x}}_e = \beta(x - \hat{x}_e) \tag{1.19}$$

with $\beta > 0$. If we consider x as a constant, i.e., x is in the steady-state x_e, because of $\beta > 0$ (negative eigenvalue), the estimate $\hat{x}_{ei}$ will finally converge to x. In practical, x

can be slowly changed due to slow load variations. For this situation, quasi-steady state approximation that treats x as a constant is a valid approach.

Therefore, the objectives of thesis are:

- Introduce the power systems modeling, its dynamic stability and bifurcation analysis.
- Implement an adaptive mechanism to track equilibrium value of eq. (1.10) for the feedback control design.
- Apply the adaptive control we design for linear system eq.(1.11) with uncertain plant parameters to the real DAE system of eq. (1.1)(1.2) to stabilize the equilibrium.

The organization of the thesis is as follows. In chapter II, we present a detailed dynamic analysis of a parameter-dependent DAE system and three bifurcations are introduced. The motivation of our adaptive control responding system parameter changing is also presented. In chapter III, we review MRAC and APPC schemes for a linear system with uncertainly system parameters. Associated mathematical proofs of Lyapunouve stability are also provided. In chapter IV, we present a dynamic equilibrium tracking mechanism to obtain the equilibrium value for uncertain or changing operating condition and apply the technique of MRAC and APPC for power systems to stabilize the equilibrium. Examples are given to demonstrate our approaches. In chapter V, conclusions are presented.

CHAPTER II

DYNAMICS OF DIFFERENTIAL-ALGEBRAIC EQUATION

In this chapter, the power system dynamics model with algebraic constraints in the form of power flow equations is studied here as differential-algebraic system (DAE). Linearization is used to get a linear ODE (original differential equations) model and then the dynamic analysis is presented through its eigenvalue analysis. We also discuss the bifurcations due to system parameters changing. Finally, according to the above analysis, we introduce our motivation to adaptive control to improving the system's dynamic and stabilizing the existing equilibrium without changing the original equilibrium value.

2.1 Modeling of Power Systems

Parameter dependent DAE of the form

$$\dot{x} = f(x, y, p) \qquad f : \Re^{n+m+q} \to \Re^{n} \tag{2.1}$$

$$0 = g(x, y, p) \qquad g : \Re^{n+m+q} \to \Re^{m} \tag{2.2}$$

$$x \in X \subset \Re^{n},\ y \in Y \subset \Re^{m},\ p \in P \subset \Re^{q}$$

is widely used to model the dynamics of power system [3][4][14]. In the parameter- state space of X, Y, P, x is a vector of n state variables, y is a vector of m algebraic states and p is a vector of q parameter variables. The m algebraic equations (2.2) define a $n+k$ dimension manifold, called constraint manifold, in the $n+m+k$ dimensional parameter-state space of X, Y, P. System equilibrium points (x_e, y_e) satisfying,

$$\begin{aligned} 0 &= f(x_e, y_e, p) \\ 0 &= g(x_e, y_e, p) \end{aligned} \tag{2.3}$$

Define a k-dimensional equilibrium manifold in the state space of X, Y. Consider an equilibrium point (x_{ei}, y_{ei}, p_i) for one operation condition p_i, linearization is often used to do analysis of dynamic stability and get a local picture of dynamic behaviors around the equilibrium point (x_{ei}, y_{ei}, p_i). Define

$$\begin{aligned} \Delta x &= x - x_{ei} \\ \Delta y &= y - y_{ei} \end{aligned} \tag{2.4}$$

The linearized DAE is expressed as below,

$$\begin{bmatrix} \Delta \dot{x} \\ 0 \end{bmatrix} = J_u \begin{bmatrix} \Delta x \\ \Delta y \end{bmatrix} \tag{2.5}$$

where J_u is denoted as the unreduced Jacobian of the DAE system

$$J_u = \begin{bmatrix} f_x & f_y \\ g_x & g_y \end{bmatrix} \tag{2.6}$$

J_u depends on (x_{ei}, y_{ei}, p_i) and when g_y is nonsingular, we can eliminate Δy from (2.5) and get the reduced linear model as following:

$$\Delta \dot{x} = J_r \Delta x \tag{2.7}$$

$$J_r = [f_x - f_y g_y^{-1} g_x] \tag{2.8}$$

J_r is the reduced Jacobian matrix (RJM) of the DAE system and also depends on (x_{ei}, y_{ei}, p_i). As p changes, we solve for the system equilibrium and build the reduced

Jacobian matrix for each (x_{ei}, y_{ei}, p_i). The dynamic behaviors and stability of the equilibrium (x_{ei}, y_{ei}, p_i) can be analyzed through the eigenvalues of the reduced Jacobian matrix J_r evaluated at the equilibrium (x_{ei}, y_{ei}, p_i).

2.2 Bifurcation due to System Parameters Changing

As operating condition p varies, the equilibrium points and its corresponding eigenvalues of RJM J_r also changes. When the structure of the system such as the numbers of equilibrium points, their stability (depend on J_r) and etc. changes due to a small shift of the system parameter p, bifurcation occurs. The bifurcation points are critical points for the dynamic stability analysis of nonlinear systems. In this section, we will brief introduce the three types of bifurcations encountered in the power system dynamic: Saddle-Node Bifurcation (SNB), Singularity-Induced Bifurcation (SIB) and Hopf Bifurcation (HB)[14][15][16].

(1) SNB: Two equilibrium points coalesce and then disappear. At this point, the J_r has zero eigenvalue, i.e. it is singular.

(2) HB: Oscillatory instability is occurred. At this point, two complex conjugate eigenvalues of J_r cross the imaginary axis.

(3) SIB: g_y becomes singular such that one eigenvalue of J_r going to infinity at both sides of the singular point with opposite sign.

In the following section, we will observe the three bifurcations through two simple power system examples.

2.2.1 An example for two-bus power systems with P controller

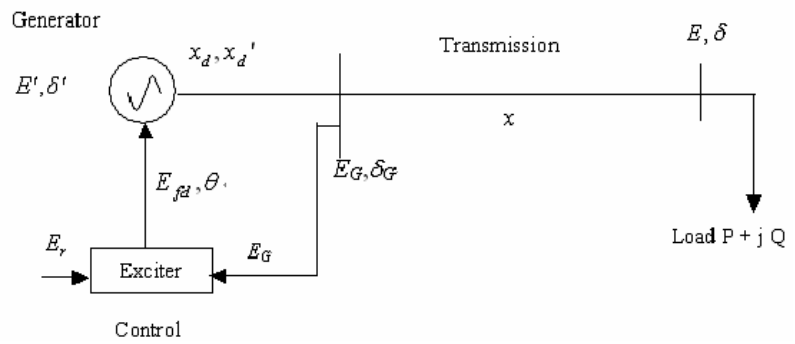

Fig. 2.1 Two-bus power system

Fig. 2.1 shows the simplified model including a one-axis generator and a first-degree simplification of the IEEE Type I excitation control. In the above the system, we assumed that the voltage dynamic is decoupled from the angle dynamic so that the angle dynamic could be ignored. We also assume that power factor of load is constant no matter load changes. Then we can get a DAE equation of the simplified model:

$$\dot{E}' = \frac{1}{T_{d0}'}\left[-\frac{x+x_d}{x'}E' + \frac{x_d - x_d'}{x'}\frac{E^2 + x'Q}{E'} + E_{fd}\right] \tag{2.9}$$

$$\dot{E}_{fd} = \frac{1}{T}\left[-(E_{fd} - E_{fd0}) - K\left(\frac{1}{E}\sqrt{(xP)^2 + (xQ + E^2)^2} - E_r\right)\right] \tag{2.10}$$

$$0 = E'^2 E^2 - (x'P)^2 - (x'Q + E^2)^2 \tag{2.11}$$

with coefficient

$$T_{d0}'=5,\ T=1.5,\ E_{fd0}=1.6,\ x_d=1.2,\ x_d'=0.2,$$
$$x=0.1,\ x'=x+x_d',\ Q=0.5P,\ E_r=1.0, K=3.2$$

E_r is the set-point voltage, E_{fdo} is the nominal field excitation, and K is control coefficients. Equation (2.11) denotes the power flow of the system, (2.9) for generator dynamic and (2.10) for the exciter dynamic. The system parameter *p* can be the load *p*={*P*, *Q*}. This is a parameter-dependent DAE model with two first-order differential equations and one algebraic constraint.

The dynamic stability of the system (2.9)-(2.11) depends on eigenvalues of reduced matrix J_r for the different load *p*.

(1) Eigenvalue analysis

Let

$$f_1(E', E_{fd}, E, P)=\frac{1}{T_{d0}'}\left[-\frac{x+x_d}{x'}E'+\frac{x_d-x_d'}{x'}\frac{E^2+x'Q}{E'}+E_{fd}\right] \tag{2.12}$$

$$f_2(E', E_{fd}, E, P)=\frac{1}{T}\left[-(E_{fd}-E_{fd0})-K\left(\frac{1}{E}\sqrt{(xP)^2+(xQ+E^2)^2}-E_r\right)\right] \tag{2.13}$$

$$g(E', E_{fd}, E, P)=E'^2E^2-(x'P)^2-(x'Q+E^2)^2 \tag{2.14}$$

The reduced Jacobian matrix of the DAE systems is

$$J_r=[f_x-f_y g_y^{-1} g_x] \tag{2.15}$$

Where

$$f_x = \begin{bmatrix} \frac{\partial f_1}{\partial E'} & \frac{\partial f_1}{\partial E_{fd}} \\ \frac{\partial f_2}{\partial E'} & \frac{\partial f_2}{\partial E_{fd}} \end{bmatrix} \tag{2.16}$$

$$f_y = \begin{bmatrix} \frac{\partial f_1}{\partial E} \\ \frac{\partial f_2}{\partial E'} \end{bmatrix} \tag{2.17}$$

$$g_x = \begin{bmatrix} \frac{\partial g}{\partial E'} & \frac{\partial g}{\partial E_{fd}} \end{bmatrix} \tag{2.18}$$

$$g_y = \begin{bmatrix} \frac{\partial g}{\partial E} \end{bmatrix} \tag{2.19}$$

J_r is a 2×2 dimensional matrix depend on $p = \{P, Q\}$. For each constant power load $p_i = \{P_i, Q_i\}$, we set equations f_1, f_2, g to zeros and resolve the three algebraic equations to find the system equilibrium values. Then we compute eigenvalues of J_r at each of equilibrium points to determine the stability of the equilibrium point.

(2) Simulation results

Starting with equilibrium tracking, as the load active power P increase, we have the associated $P-V$ curve shown in Fig. 2.2.

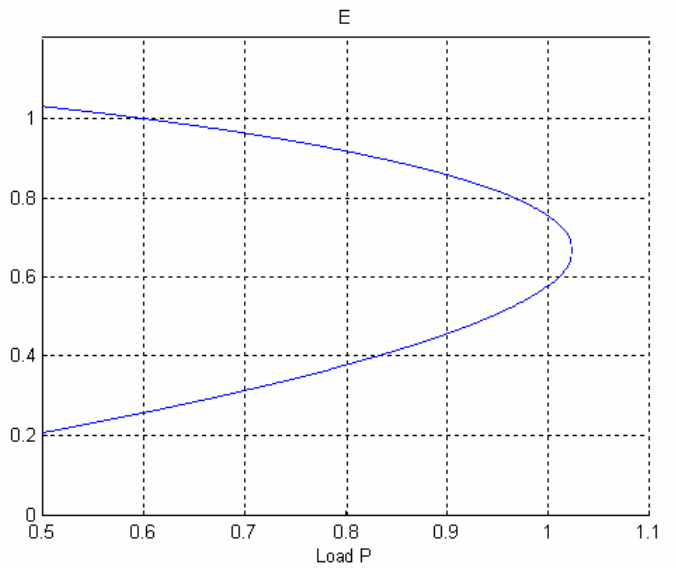

Fig. 2.2 PV curve for two-bus power system

For each $p_i = \{P_i, Q_i\}$, nonlinear systems may have one or more than one or no equilibrium points. In the case, when $0 \le P < 1.0242$, the system has two equilibria; when $P = 1.0242$, one equilibria; and no equilibria when $P > 1.0242$. We will observe the bifurcations through the eigenvalue analysis along the $P - V$ curve.

Fig. 2.3 shows two eigenvalues of the upper higher bus voltage part of $P - V$ curve. The dotted line represents the real part of the eigenvalues while the other line represents the imaginary parts. From the below figure, we could know that when P increases from 0.995 to 0.996, the pairs of complex conjugate eigenvalues cross the imaginary axis in the complex plane from left to right. This type of oscillatory instability is associated with Hoph bifurcation (HB).

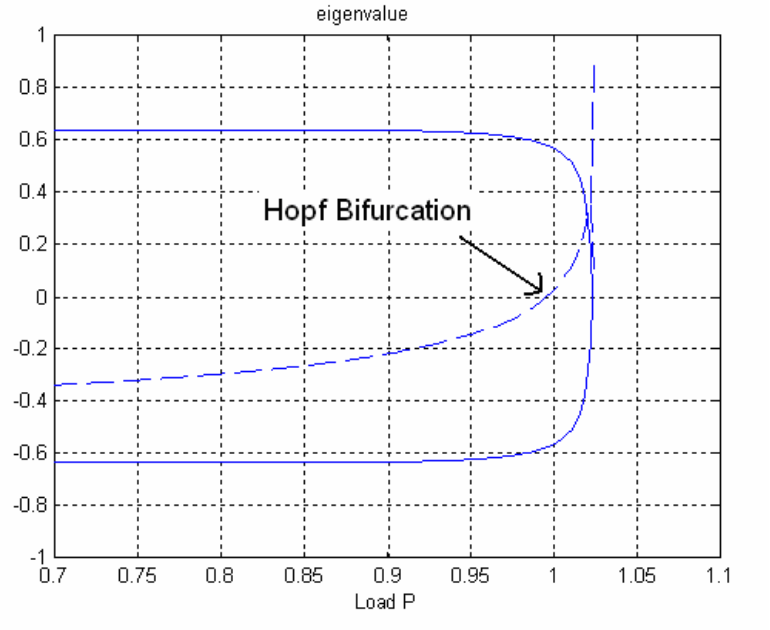

Fig. 2.3 Eigenvalues of upper bus voltage on the PV curve

Fig. 2.4 shows two eigenvalues of the below lower bus voltage part of $P-V$ curve. The dotted line represents one eigenvalues whi\le the other line represents another negative eigenvalue. Both of the two eigenvalues are real numbers without imaginary parts.

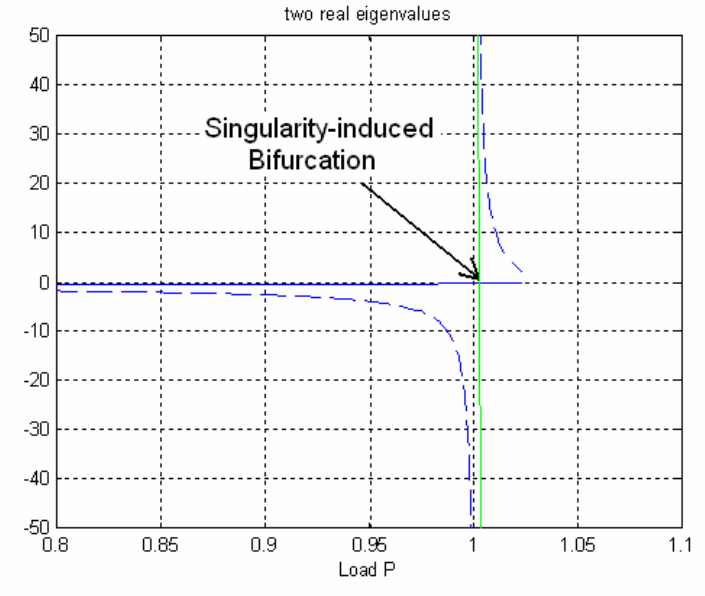

Fig. 2.4 Eigenvalues of lower bus voltage on the PV curve

From the above figure, we see clearly that one eigenvalue of J_r tends to minus infinity as P close to 1.001 from one side, say $P = 1.001^-$; as $P = 1.001$, g_y is singular, after this point, say $P = 1.001^+$, the eigenvalue of J_r tends to plus infinity. Thus, the system changes the property at $P = 1.001$ and it corresponds to singularity-induced bifurcation (SIB).

We draw the $P-V$ curve again with the three bifurcation points in Fig. 2.5. As P changes, we obtain three bifurcation points A, B and C based on the RJM J_r. A represents Hopf Bifurcation and C represents singularity- induced bifurcation.

We can also observe another bifurcation, saddle-node bifurcation (SNB) in this case. As $P < 1.0242^-$, two equilibrium points exists. As $P > 1.0242^+$, no equilibrium point

exists anymore. It therefore can be inferred that at $P \cong 1.0242$, the two equilibrium points coalesce and then disappear on the tip of the $P-V$ curve. At this point, one eigenvalue approaches and finally becomes zeros, i.e. J_r is singular. After the point B, no power flow solutions exist anymore and results in voltage collapse [3][14].

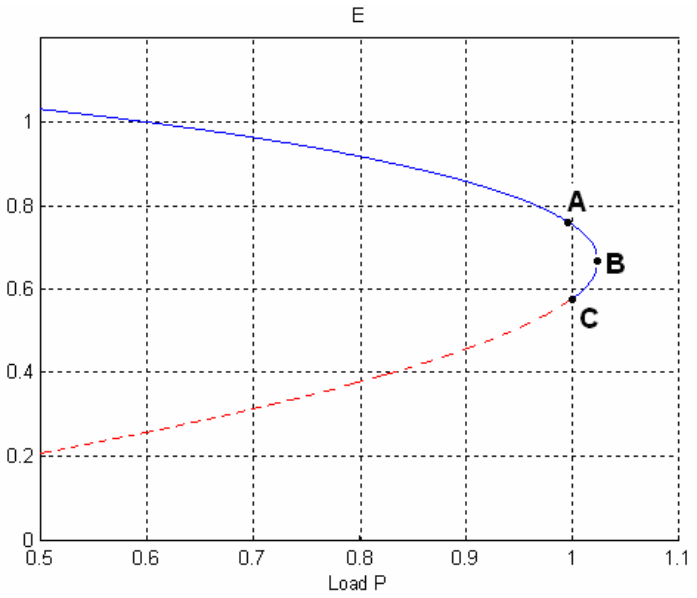

Fig. 2.5 PV curve for K=3.2

In Fig. 2.5, the dotted line on the lower bus voltage of the $P-V$ curve, is stable but typically not viable because of too low bus voltage for operation. We should let the power system to operate in a practical region on the upper part of the $P-V$ curve. As addressed in [14], it could be observed that the region of the attraction of a stable equilibrium, the usual operating point, shrinks as the load increases and disappears when Hopf Bifurcation A is crossed. In such situation, we would change system parameters of

the excitation system or the transmission part to relocate the bifurcation points, thus improves the system dynamic properties. For examples of the same DAE systems (2.9)-(2.10), if we only change control coefficients K of (2.10) from 3.2 to 5.0 and remain the rest coefficient T_{d0}', T, E_{fd0}, x_d, x_d', x, x', E_r with the same value, we have another $P-V$ curve for K=5 shown as Figure 2.6.

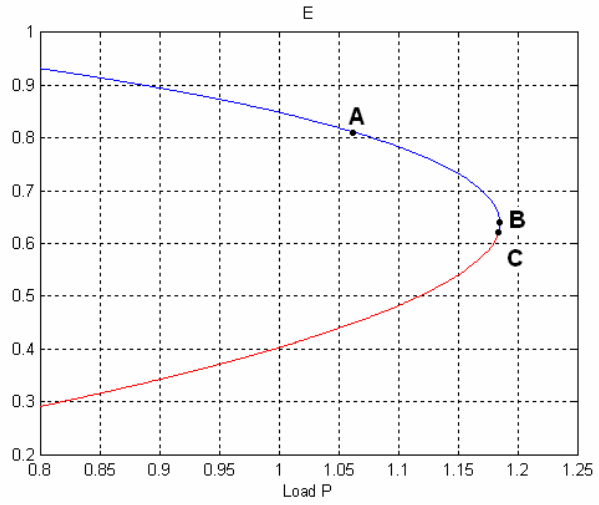

Fig. 2.6 PV curve for K=5

Comparing Fig. 2.6 with Fig. 2.5, Hoph Bifurcation A is to be pushed from lower load $P \cong 0.995$ to higher load $P \cong 1.062$ as K increasing from 3.2 to 5.0.

It seems that we can easily increase the system's loadability by increasing the control coefficient K. However, as K increases, imaginary part of eigenvalue of Jacobin matrix also increases. It makes the larger overshoot and is easier to over the system or equipment's capacity and damage the system. In Fig. 2.7, the dotted line shows the

imaginary parts of eigenvalue for K =3.2; the other line, for K =5. It is clear that when K =5, the value of the imaginary part is larger than those when K =3.2.

Therefore, we'd like to design an extra controller which can change the dynamic properties between the segment A-B to increase the system's loadability without adjusting the coefficient K .

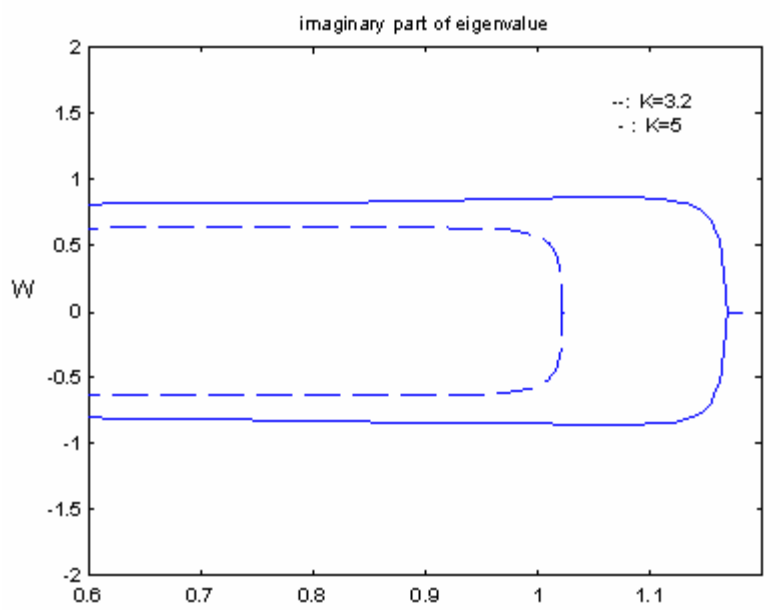

Fig. 2.7 Imaginary value of eigenvalues for P control with different K

There is also another method: increasing excitation voltage to increase loadability. This way, however, results in some disadvantage: too high bus voltage when the low load. See Fig. 2.8. The dotted line represents the PV curve when the nominal field excitation $E_{fdo} = 2.0$ while the other present $E_{fdo} = 1.6$. When $E_{fdo} = 2.0$, voltage is too

high for normal operation in the low load condition.

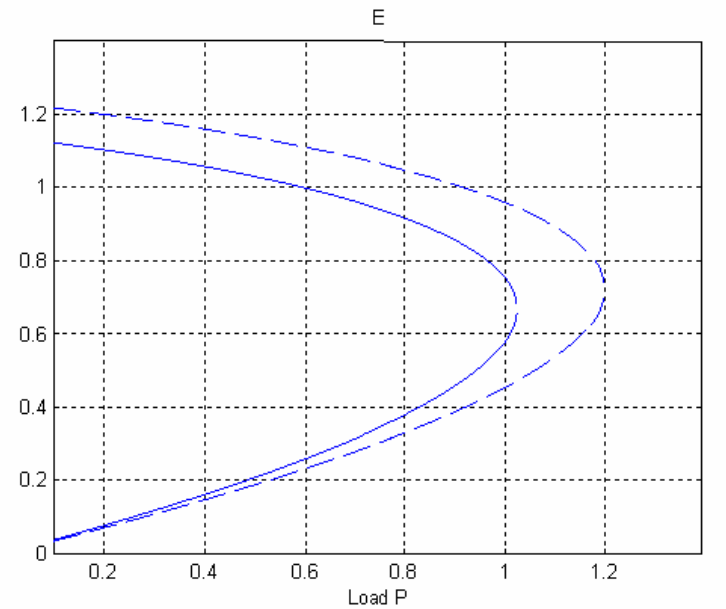

Fig. 2.8 PV curve for $E_{fdo} = 2.0$ **and** $E_{fdo} = 1.6$

From Fig. 2.7 and Fig. 2.8, we know that sometimes, we can increase the system's loadability directly by resetting the operation parameters such as control coeffiecient or set-points. Those ways, however, would change the original PV curve and cause some problems. For example, increasing control coefficient K makes increasing loadability while it also increases imaginary value of eigenvalue where it often can be referred as shrinking the 'safe' stability region. Therefore, we would design an extra control to change the system's dynamic to increase loadability without changing the original PV curve.

2.2.2 Another example for two-bus power systems with PI controller

Let us consider the similar 2-bus power system of section 2.2.1 except for that excitation control becomes PI controller.

$$\dot{E}' = \frac{1}{T_{d0}'}\left[-\frac{x+x_d}{x'}E' + \frac{x_d - x_d'}{x'}\frac{E^2 + x'Q}{E'} + E_{fd}\right] \tag{2.20}$$

$$\dot{E}_{fd} = \frac{1}{T}\left[-(E_{fd} - E_{fd0} - \Delta E_{fd0}) - K(E_g - E_r)\right] \tag{2.21}$$

$$\dot{\Delta E}_{fd} = \gamma(E_r - E_g) \tag{2.22}$$

$$0 = E'^2E^2 - (x'P)^2 - (x'Q + E^2)^2 \tag{2.23}$$

With coefficient

$$T_{d0}' = 5,\ T = 1.5,\ E_{fd0} = 1.6,\ x_d = 1.2,\ x_d' = 0.2,$$
$$x = 0.1,\ x' = x + x_d',\ Q = 0.5P,\ E_r = 1.0, K = 3.2,\ \gamma = 0.1$$

where $E_g = \frac{1}{E}\sqrt{(xP)^2 + (xQ + E^2)^2}$, $\gamma = 0.1$, and the rest coefficients is the same as those in the former section.

Similarly, we do eigenvalue and bifurcation analysis and get its PV curve and bifurcation points as in Fig. 2.9.

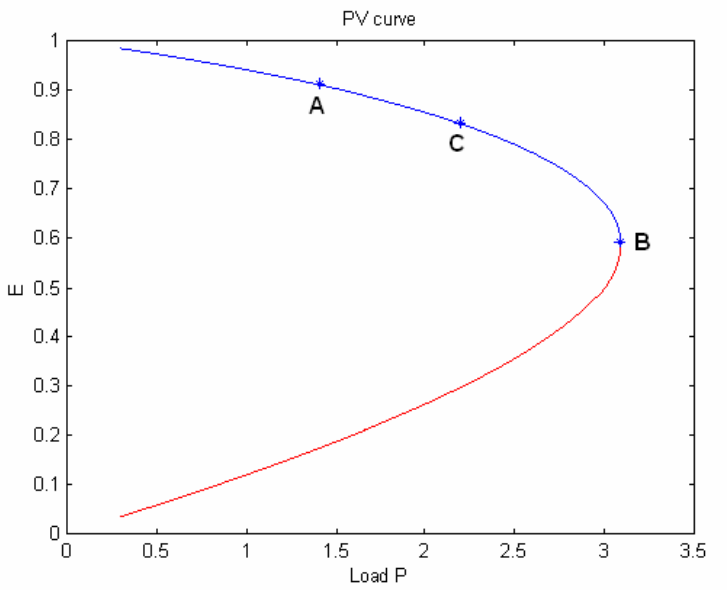

Fig. 2.9 PV curve for PI control K=3.2

For the parameter-dependent DAE system (2.20)-(2.23), it also has three bifurcations: Hopf bifurcation (point A), Saddle-Node Bifurcation (point B) and Singularity-Induced Bifurcation (point C). Before Saddle-node Bifurcation B, the system has two equilibrium points; after B, the equilibrium no longer exists. Loadability of the system is at Hopf Bifurcation A ($P \cong 1.39$). If the load $P < 1.39$, the system's equilibrium in the upper part of the PV curve is stable; otherwise, it is unstable. Besides, the Singularity-induced Bifurcation C is moved from the lower part to the upper part of PV curve and located between A and B.

Similar with the example in the section 2.2.1, we can increase control coefficient K from 3.2 to 5.0 and get a new PV curve as below Fig. 2.10. Since the equilibrium value of E_g , E_{ge} , is always equal to one and independent of K , the shapes of PV curve in

Fig. 2.9 and Fig. 2.10 are totally identical. The location of point B and C are unchanged as well. The point A, however, is pushed to higher load $P \cong 1.402$. Thus, just like the former example, we can also increase the system's loadability by increasing control coefficient K. This similar method, however, cause the similar problem: making the imaginary part of eigenvalue increasing and therefore weakening the system's dynamic properties. See Fig. 2.11.

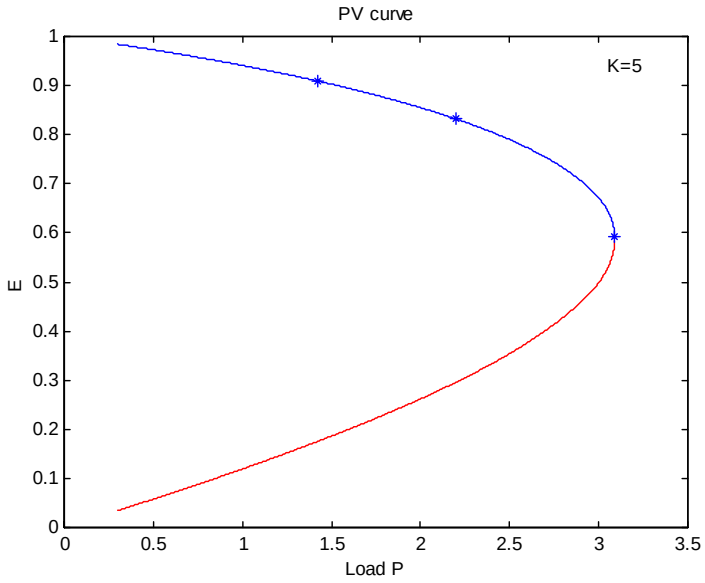

Fig. 2.10 PV curve for PI control K=5.0

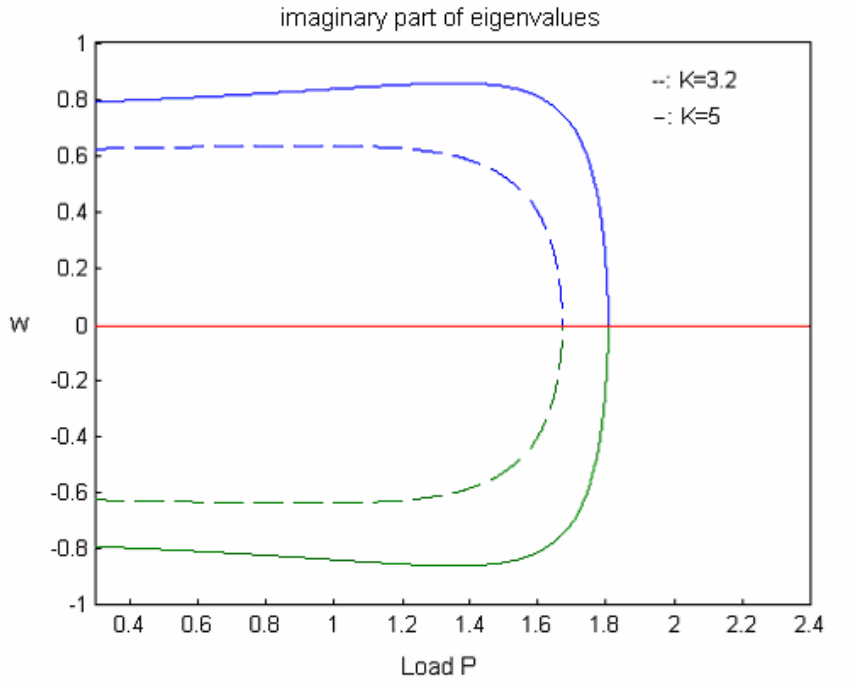

Fig. 2.11 Imaginary value of eigenvalues for PI control with different K

As a result, we would like to design an extra control to stabilize the segment A-B and push A to the higher load without changing the control coefficients or the set-point.

2.3. An Example for an Adapting P Control

As we discuss the two bus system in section 2.2.1, at the low power load, we prefer a small control coefficient K to let the linearized system with the eigenvalues of small imaginary part, while as power load increasing, we require a large coefficient K to

increase the system's loadability. Therefore, as power load vary with time, we can design an adapting P control for adapting power load change. The following Table I shows the HB (the system's loadability) and SNB for different K. Fig. 2.12 shows an adapting P control designed for different load according to Table I and Fig. 2.13 shows the block diagram of the system with the adapting control.

Table I Pre-computed Look-up Table for HB and SNB for Different K

K	2.5	3	4	5	8	12
SNB	0.9424	0.9935	1.09	1.1842	1.359	1.563
HB	0.9359	0.9752	1.072	1.0842	1.1716	1.2355

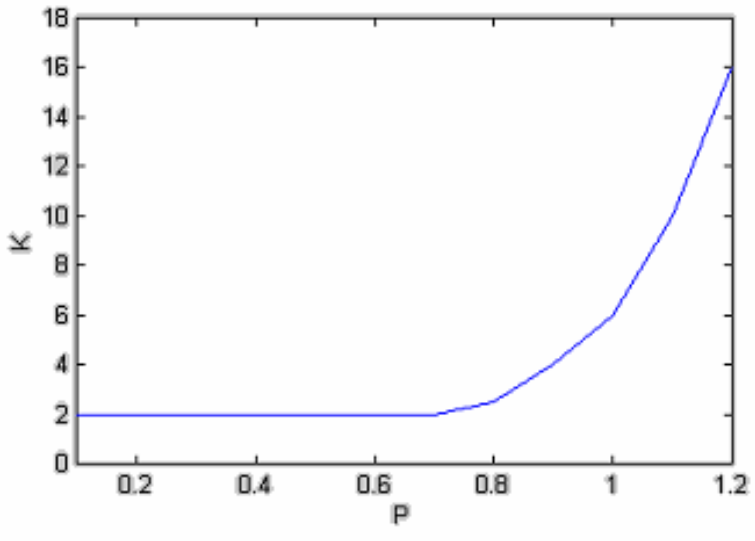

Fig. 2.12 Adapting P Control

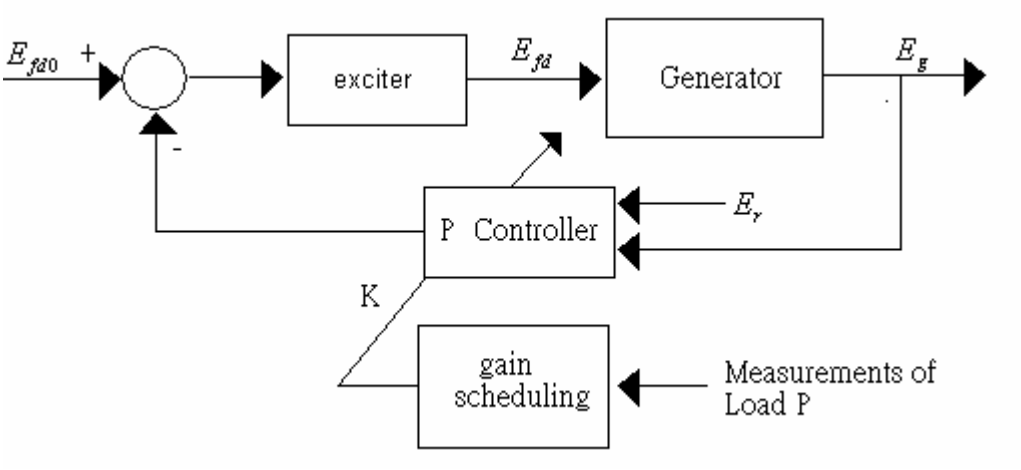

Fig. 2.13 Block diagram for the adapting P control

The above adapting control is a kind of gain-scheduling controller. It has advantages of higher loadability without weakening its dynamic properties at low load compared to the constant P control. The adjustment mechanism of the gain-scheduling controller, however, is precomputed off-line and therefore, there is no feedback compensation for incorrect schedules (it could be resulted from imprecise coefficient). This may lead to deterioration of performance [10]. Thus, we would like to design an adaptive control which can sense the unstable condition online (trajectories would diverge from the equilibrium manifold) to improve the dynamic stability and robustness of the original system. Following, we start our motivation to our adaptive control.

2.4. Motivation for the On-Line Adaptive Control

From section 2.2, we know that the segment A-B (see Fig. 2.5 or Fig. 2.6) is unstable equilibrium because of the unstable matrix J_r. However, power flow solution still exists (the system still have the equilibrium). Therefore, we can design an extra control to stabilize the unstable equilibrium.

Take the same example of eq. (2.9)-(2.11) for which K=3.2 and load $P = 1.0$. We resolve algebraic equation (2.) so that we can find the equilibrium value: $E_e^{'} = 1.0257$, $E_{fde} = 2.1826$ and then compute its reduced Jacobian matrix J_r as follows,

$$J_r = \begin{bmatrix} 0.8331 & 0.2 \\ -4.1156 & -0.6667 \end{bmatrix} \tag{2.24}$$

Because the eigenvalues of (2.24), $\lambda = 0.0832 \pm 0.5107\,j$, the equilibrium E'=1.0257, $E_{fd} = 2.1826$ is unstable. Rewrite the linear ODE equation with the extra control input Δu_p and output ΔE_g, we have

$$\Delta \dot{x} = A_i \Delta x + B_i \Delta u_p \tag{2.25}$$

$$\Delta E_g = C_i \Delta x \tag{2.26}$$

where

$$A_i = J_r = \begin{bmatrix} 0.8331 & 0.2 \\ -4.1156 & -0.6667 \end{bmatrix}, \quad B_i = \begin{bmatrix} 0 \\ 0.67 \end{bmatrix}, \quad C_i = \begin{bmatrix} 1.8213 & 0 \end{bmatrix}$$

$$\Delta \dot{x} = \begin{bmatrix} \Delta E' \\ \Delta E_{fd} \end{bmatrix} \tag{2.27}$$

For the linear system (2.25) (2.26), we can easily design a feedback control $\Delta u_p = H(\Delta x)$ or $\Delta u_p = H(\Delta E_g)$ by classical linear control theorem to stabilize the equilibrium. It should be known that in the steady-state, $\Delta u_p = 0$ because of $\Delta x = 0$, therefore we just stabilize the system but do not change the original equilibrium value.

Next, we would deal with the situation when the load is uncertain between the segment A-B or the load is slowly changing.

Since the trajectories would diverge away from the unstable equilibrium A-B, we can design an auxiliary adaptive controller which can sense the diverged trajectories from its equilibrium and then apply an appropriate feedback control signal to stabilize J_r. By the auxiliary feedback controller, we could make the unstable equilibrium segment A-B become stable without changing the original $P-V$ curve and therefore increases the system's loadability.

Let's rewrite (2.1) (2.2) with a input signal u

$$\dot{x} = f(x, y, u, p_i) \tag{2.28}$$
$$0 = g(x, y, u, p_i) \tag{2.29}$$

Since the standard stabilization problem is defined as stabilization of an equilibrium point at the origin, we can change variables with respect to an arbitrary operating condition (p_i, u_{ss}), which includes its steady-state input u_{ss} referred as a set-point or reference input.

For each system operation condition (p_i, u_{ss}), its corresponding equilibrium point is satisfying

$$\begin{aligned} 0 &= f(x_{ei}, y_{ei}, p_i, u_{ss}) \\ 0 &= g(x_{ei}, y_{ei}, p_i, u_{ss}) \end{aligned} \tag{2.30}$$

Define

$$\begin{aligned} \Delta x &= x - x_{ei} \\ \Delta y &= y - y_{ei} \\ \Delta u &= u - u_{ss} \end{aligned} \tag{2.31}$$

Then we get a linearized model as,

$$\begin{bmatrix} \Delta \dot{x} \\ 0 \end{bmatrix} = \begin{bmatrix} f_x & f_y \\ g_x & g_y \end{bmatrix} \begin{bmatrix} \Delta x \\ \Delta y \end{bmatrix} + \begin{bmatrix} f_u \\ g_u \end{bmatrix} \Delta u \tag{2.32}$$

Similarly, if g_y is nonsingular, we can eliminate Δy from (2.32) and get a reduced linear model

$$\Delta \dot{x} = A_i \Delta x + B_i \Delta u \tag{2.33}$$

where

$$A_i = [f_x - f_y g_y^{-1} g_x] \tag{2.34}$$

$$B_i = [f_u - f_y g_y^{-1} g_u] \tag{2.35}$$

If we set $\Delta u \equiv 0$, equation (2.33) becomes our original linearized systems (2.7), i.e.,

$$\Delta \dot{x} = A_i \Delta x = J_r \Delta x$$

Without feedback control Δu, the dynamic stability of one equilibrium (x_{ei}, y_{ei}) depends only on $A_i = J_r$. Since A_i changes as operation condition (p, u) varies,

A_i could be also referred to as a function of the parameter (p,u). As the system goes through different operating conditions, the parameter (p,u) change leads to different value for A_i . For the power systems, A_i may be a stable matrix for some parameter (p_i,u_{ss}) while unstable for another (p_j,u_{ss}). For example in the section 2.2.1 of Figure 2.5, segment A-B is unstable. Therefore, the system is unstable for load $0.996 < P < 1.024$.

For a given and known (p_i,u_{ss}), A_i,B_i can be calculated exactly and therefore it's is easy to design feedback control law Δu and resolve stability problems for the linear system (2.33) by classic linear control techniques as we discuss in the section at first. In the thesis, however, (p_i,u_{ss}) is assumed to be uncertain or changing system parameters and thus we would propose some linear adaptive schemes to estimate A_i , B_i of the unknown linear system (2.33) and apply an extra auxiliary feedback control signal $\Delta u = -h(\Delta x, A_i, B_i)$ such that the origin $\Delta x = 0$ become uniformly asymptotically stable equilibrium points of the closed-loop system (2.36).

$$\Delta \dot{x} = A_i \Delta x - B_i h(\Delta x, A_i, B_i) \tag{2.36}$$

If only output Δy_p is available for measurement, we replace (2.36) by

$$\Delta \dot{x} = A_i \Delta x - B_i h(\Delta y_p, A_i, B_i) \tag{2.37}$$

Fig. 2.14 is the diagram showed our motivation to the adaptive control design.

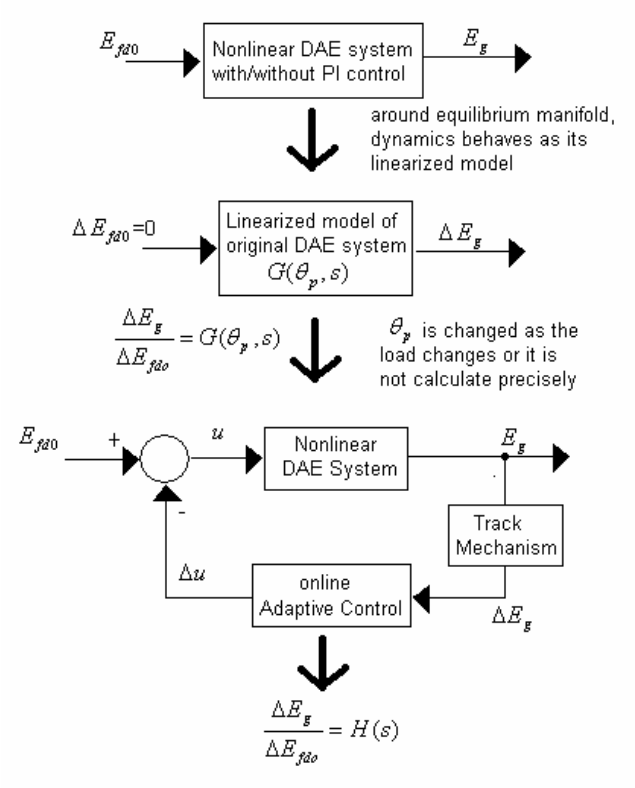

Fig. 2.14 Diagram for motivation to the adaptive control

It should be noticed that Δu is designed as an extra feedback control of the state Δx or the measurable output Δy_p. The overall control signal $u = \Delta u + u_{ss}$ has a feedback component Δu and a feedforward component u_{ss}.

The above approach requires the knowledge of the equilibrium value x_{ei} since the feedback control signal $\Delta u = -h(\Delta x) = -h((x - x_{ei}))$ must calculated in terms of x_{ei}. However, the equilibrium x_{ei} would vary as operating condition p_i changes and therefore is unavailable.

In the Chapter III, we consider the linear system with unknown system

parameter A_i, B_i (2.38) and propose the linear MRAC and APPC schemes to solve the stability problem of the origin $\Delta x_e = 0$.

The linear system is describe as

$$\Delta \dot{x} = A_i \Delta x + B_i \Delta u_p \tag{2.38}$$

or

$$\Delta \dot{x} = A_i \Delta x + B_i \Delta u_p \tag{2.39}$$

$$\Delta y_p = C_i \Delta x \tag{2.40}$$

where Δy_p is a measurable output and A_i, B_i, C_i are uncertain system parameters.

In the Chapter IV, we apply our adaptive control approaches to the real DAE system. We would resolve the problem of the unknown x_{ei} by implementing an adaptive mechanism to track x_{ei} and apply MRAC or APPC to stabilize x_{ei}.

CHAPTER III

ADAPTIVE CONTROL FOR LINEAR SYSTEMS

For more than two decades, adaptive control research has exclusively dealt with linear systems and has developed controllers which guarantee global boundedness and tracking[9][10]. In this chapter, we will introduce two popular linear adaptive control schemes: Model Reference Adaptive Control (MRAC) and Adaptive Pole Placement (APPC) designed for the linear system with uncertainty parameters. The design procedures combine a control law whose form is the same as we use in the known parameter case with an adaptive law that provides on-line estimates for the controller parameters. The proofs of the Lypunouve stability of the systems are also provided.

3.1 Model Reference Adaptive Control

Model Reference Adaptive Control (MRAC) is one of the main approaches to adaptive control. The basic structure of MRAC is shown in Fig.3.1.

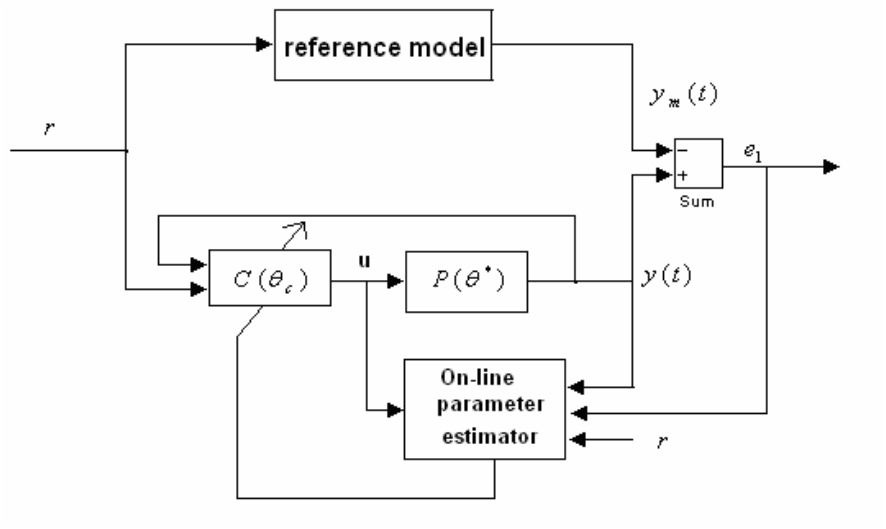

Fig. 3.1 Block diagram of model reference adaptive control

The reference model is chosen to generate the desired trajectory y_m, which the output y has to follow. The tracking error $e_1 = y - y_m$ represents the deviation of the output y from the desired y_m. The closed-loop system is made up of a feedback control law that contains controller $C(\theta_c)$ and an adjustment mechanism that generates the controller parameter estimates $\theta_c(t)$ on-line.

3.1.1 Problem statement and assumption

In this section, we describe the problems that we would deal with and make some assumption for the following control design.

Consider the SISO, linear time-invariant (LTI) system described by the vector

differential equation,

$$\dot{x}_p = A_p x_p + B_p u_p \tag{3.1}$$

$$y_p = C_p^T x_p \tag{3.2}$$

where $x_p \in \Re^n, y_p, u_p \in \Re^1$ and A_p, B_p, C_p have the appropriate dimensions. The transfer function of the linear system is given by (3.3).

$$y_p = G_p(s) u_p \tag{3.3}$$

$$G_p(s) = k_p \frac{Z_p(s)}{R_p(s)} = C_p^T (sI - A_p)^{-1} B_p \tag{3.4}$$

where R_p, Z_p are monic polynomials and k_p is a constant referred as the high frequency gain [10].

The reference model, selected by the designer to describe the desired characteristics of the system, is describe by

$$\dot{x}_m = A_m x_m + B_m r \tag{3.5}$$

$$y_m = C_m^T x_m \tag{3.6}$$

where r is the reference input which is assumed to be a uniformly bounded and piecewise continuous function of time. The transfer function of the reference model given by

$$y_m = W_m(s) r \tag{3.7}$$

$$W_m(s) = k_m \frac{Z_m(s)}{R_m(s)} = C_m^T (sI - A_m)^{-1} B_m \tag{3.8}$$

where R_m, Z_m are monic polynomials and k_m is a constant.

The MRC objective is to design the control input u_p so that all signals are bounded and the output y_p tracks the reference model output y_m for any given reference input r. In order to meet the MRC and the following MRAC objectives, we assume that the linear system $G_p(s)$ and the reference model $W_m(s)$ satisfy the following assumptions:

(1) $G_p(s)$ Assumptions

P1. $z_p(s)$ is a monic Hurwitz, polynomial of degree m_p.

P2. The sign of the high-frequency gain k_p is known.

P3. The relative degree $n^* = n_p - m_p$ of $G_p(s)$ is known. n_p is degree of $R_p(s)$.

P1 requires that $G_p(s)$ to be minimum phase, i.e, the real parts of all zeros of $G_p(s)$ are negative while stable poles are not required. We also allowed that the plant to be uncontrollable or unobservable i.e., we allow $G_p(s)$ has common stable zeros and poles.

(2) $W_m(s)$ Assumptions

M1. $R_m(s), Z_m(s)$ are monic Hurwitz polynomials of degree p_m, q_m ,respectively, and $p_m \le n$

M2. The relative degree $n_m^* = p_m - q_m$ of $W_m(s)$ is equal to n^*

3.1.2 MRC schemes for the plant with known parameters

For a linear plant with exactly known parameters, the MRC objectives is met if control signal u_p is chosen so that the closed-loop transfer function r to y_p has stable poles and is equal to reference model $W_m(s)$. A trivial choice for u_p is the cascade open-loop control law

$$u_p = C(s)r \tag{3.9}$$

$$C(s) = \frac{W_m(s)}{G_p(s)} = \frac{k_m}{k_p}\frac{Z_m(s)R_p(s)}{R_m(s)Z_p(s)} \tag{3.10}$$

which leads to the closed-loop transfer function

$$\frac{y_p}{r} = C(s)G_p(s) = W_m(s) \tag{3.11}$$

This control law, however, is feasible only when $z_p(s)$ is a Hurwitz. Otherwise, may involve unstable zero-pole cancellation, which will lead to unbounded internal states [9][10].

Let us consider feedback control law

$$u_p = \theta_1^{*T}\frac{\alpha(s)}{\Lambda(s)}u_p + \theta_2^{*T}\frac{\alpha(s)}{\Lambda(s)}y_p + \theta_3^* y_p + c_0^* r \tag{3.12}$$

shown in Fig 3.2 where

$$\alpha(s) = [s^{n-2}, s^{n-3}, ..., s, 1]^T \quad \text{for} \quad n \geq 2$$
$$\alpha(s) = 0 \quad \text{for} \quad n = 1$$

$\theta_1^*, \theta_2^* \in R^{n-1}, \theta_3^*, c_0^* \in R^1$ are constant parameters to be designed and $\Lambda(s)$ is an arbitrary monic Hurwitz polynomial of degree n-1 that contains $Z_m(s)$ as a factor, i.e.,

$$\Lambda(s) = Z_m(s)\Lambda_0(s) \tag{3.13}$$

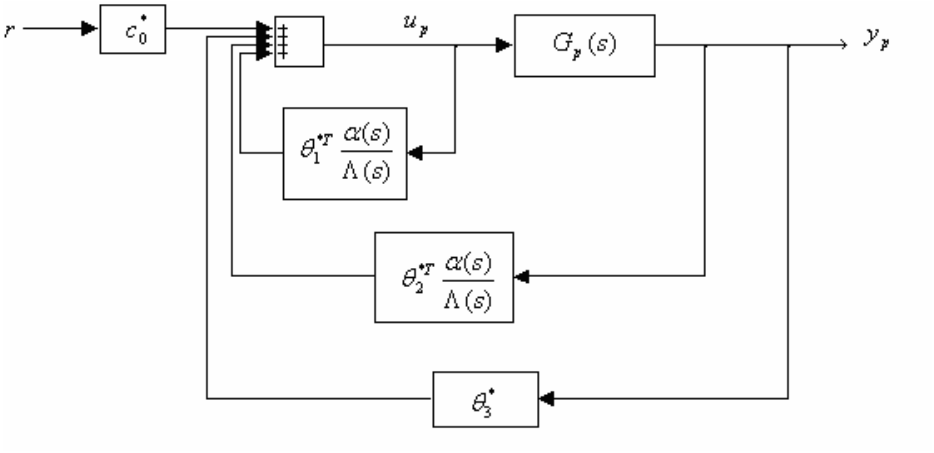

Fig. 3.2 Block diagram of model reference control

The control parameter vector $\theta^* = [\theta_1^{*T}, \theta_2^{*T}, \theta_3^*, C_0^*]^T \in R^{2n}$ is to be chosen so that the transfer function from r to y_p is equal to $W_m(s)$.

The I/O properties of the closed-loop plant shown in Figure1 are described by the transfer function equation

$$y_p = G_c(s)r \tag{3.14}$$

$$G_c(s) = \frac{c_0^* k_p Z_p \Lambda^2}{\Lambda[(\Lambda - \theta_1^{*T}\alpha(s))R_p - k_p Z_p(\theta_2^{*T}\alpha(s) + \theta_3^{*T}\Lambda)]} \tag{3.15}$$

We select the controller parameter $\theta^* = [\theta_1^{*T}, \theta_2^{*T}, \theta_3^*, c_0^*]^T$ so that the closed-loop poles are stable and the transfer function $G_c(s) = W_m(s)$.

Let

$$c_0^* = \frac{k_m}{k_p} \tag{3.16}$$

By using $\Lambda(s) = Z_m(s)\Lambda_0(s)$, we should have

$$(\Lambda - \theta_1^{*T}\alpha(s))R_p - k_p Z_p(\theta_2^{*T}\alpha(s) + \theta_3^{*T}\Lambda) = Z_p\Lambda_0 R_m \tag{3.17}$$

We can express (3.17) in terms of the algebraic equation (3.18) [6].

$$S\bar{\theta}^* = p \tag{3.18}$$

where $\bar{\theta}^* = [\theta_1^{*T}, \theta_2^{*T}, \theta_3^*]^T$, S is an $(n + n_p - 1) \times (2n - 1)$ matrix that depends on the coefficients of R_p, k_p, Z_p and Λ, and p is an $(n + n_p - 1)$ vector with the coefficients of $\Lambda R_p - Z_p\Lambda_0 R_m$. The existence of $\bar{\theta}^*$ depends on the properties of the matrix S. For example, if $n_p = n$ and S is nonsingular, (3.18) will have one unique solution. We will demonstrate the approach by the following example 3.1.2.

We begin with the following state-space realization of the control law eq. (3.12)

$$\dot{w}_1 = Fw_1 + gu_p \tag{3.19}$$

$$\dot{w}_2 = Fw_2 + gy_p \tag{3.20}$$

$$u_p = \theta^{*T} w \tag{3.21}$$

Where $w_1, w_2 \in \Re^{n-1}$,

$$w = [w_1^T, w_2^T, y_p, r]^T, \quad \theta^* = [\theta_1^{*T}, \theta_2^{*T}, \theta_3^*, C_0^*]^T \tag{3.22}$$

$$F = \begin{bmatrix} -\lambda_{n-2} & -\lambda_{n-3} & -\lambda_{n-3} & \dots & -\lambda_0 \\ 1 & 0 & 0 & \dots & 0 \\ 0 & 1 & 0 & \dots & 0 \\ \vdots & \vdots & \vdots & \vdots & \vdots \\ 0 & 0 & 0 & 1 & 0 \end{bmatrix}, \quad g = \begin{bmatrix} 1 \\ 0 \\ 0 \\ \vdots \\ 0 \end{bmatrix} \tag{3.23}$$

λ_i are coefficient of

$$\Lambda(s) = s^{n-1} + \lambda_{n-2}s^{n-2} + \lambda_{n-3}s^{n-3} + \dots + \lambda_1 s + \lambda_0 = \det(sI - F) \tag{3.24}$$

(F, g) is the state-space realization of $\dfrac{\alpha(s)}{\Lambda(s)}$, i.e., $(sI - F)^{-1} g = \dfrac{\alpha(s)}{\Lambda(s)}$.

We obtain the state-space representation of the overall closed-loop system by augmenting the state x_p with w_1, w_2

$$\dot{Y}_c = A_c Y_c + B_c c_o^* r \qquad Y_c(0) = Y_{c0} \tag{3.25}$$

$$y_p = C_c^T Y_c \tag{3.26}$$

Where

$$Y_c = [x_p^T, w_1^T, w_2^T] \qquad \in \Re^{n_p + 2n-2} \tag{3.27}$$

$$A_c = \begin{bmatrix} A_p + B_p\theta_3^{*T}C_P^T & B_p\theta_1^{*T} & B_p\theta_2^{*T} \\ g\theta_3^{*T}C_p^T & F + g\theta_1^{*T} & g\theta_2^{*T} \\ gC_p^T & 0 & F \end{bmatrix} \quad \in \Re^{n_p+2n-2} \times \Re^{n_p+2n-2} \tag{3.28}$$

$$B_c = \begin{bmatrix} B_p \\ g \\ 0 \end{bmatrix} \text{ and } C_c^T = [C_p^T, 0, 0] \quad \in \Re^{n_p+2n-2} \tag{3.29}$$

From (3.12), (3.15), (3.26), we establish that the transfer function from r to y_p is given by

$$\frac{y_p(s)}{r(s)} = \frac{c_0^* k_p Z_p \Lambda^2}{\Lambda[(\Lambda - \theta_1^{*T}\alpha(s))R_p - k_p Z_p(\theta_2^{*T}\alpha(s) + \theta_3^{*T}\Lambda)]} = W_m(s) \tag{3.30}$$

It implies that

$$C_c^T(sI - A_c)^{-1}B_c c_0^* = \frac{c_0^* k_p Z_p \Lambda^2}{\Lambda[(\Lambda - \theta_1^{*T}\alpha(s))R_p - k_p Z_p(\theta_2^{*T}\alpha(s) + \theta_3^{*T}\Lambda)]} = W_m(s) \tag{3.31}$$

And therefore,

$$\det(sI - A_c) = \Lambda[(\Lambda - \theta_1^{*T}\alpha(s))R_p - k_p Z_p(\theta_2^{*T}\alpha(s) + \theta_3^{*T}\Lambda)] = \Lambda z_p \Lambda_0 R_m \tag{3.32}$$

It is clear that the eigenvalues of A_c are equal to the roots of the Hurtwiz polynomials Λ, z_p, R_m and thus, A_c is a stable matrix which implies all states of A_c is bounded if bounded r.

Since the effect of initial condition, we do not guarantee $y_p(t) = y_m(t)$, but instead

that $y_p(t) \to y_m(t)$ exponentially fast with a rate that depends on the closed-loop dynamics. Following, we analyze the effect of initial conditions for the output tracking error $e_1(t) = y_p(t) - y_m(t)$

Since $C_c^T(sI - A_c)^{-1}B_c c_0^* = W_m(s)$, the reference model may be realized by the triple matrix ($A_c, B_c c_0^*, C_c$) and described by the non-minimal state space representation

$$\dot{Y}_m = A_c Y_c + B_c c_o^* r \qquad Y_m(0) = Y_{m0} \tag{3.33}$$

$$y_m = C_c^T Y_m \tag{3.34}$$

where $Y_m \in \Re^{n_p+2n-2}$

Letting $e = Y_c - Y_m$ and $e_1 = y_p - y_m$, from(3.25) (3.26), and (3.33) (3.34),

$$\dot{e} = A_c e \qquad e_1 = C_c^T e \tag{3.35}$$

We have a solution

$$e_1 = C_c^T \exp(A_c t)(Y_c(0) - Y_m(0)) \tag{3.36}$$

Because A_c is stable, $e_1(t)$ exponentially converges to zero. The rate of convergence depends on the location of the eigenvalues of A_c, which are equal to the roots of $\Lambda(s)z_p(s)\Lambda_0(s)R_m(s) = 0$. We can design $\Lambda(s)\Lambda_0(s)R_m(s)$ to have fast zeros but we are sill limited by the zeros of $z_p(s)$ which are fixed by the given plant.

(1) Example 3.1.2

Consider a linear second-order plant

$$y_p = \frac{-(s+5)}{s^2 - 2s + 1} u_p$$

And the reference model

$$y_m = \frac{3}{s+3} r$$

The order of the plant is $n_p = 2$ and the relative degree $n^* = 1$ is equal to that of the reference model. We choose the polynomial

$$\Lambda(s) = s + 1 = \Lambda_0(s)$$

and the control input

$$u_p = \theta_1^* \frac{1}{s+1} u_p + \theta_2^* \frac{1}{s+1} y_p + \theta_3^* y_p + c_0^* r$$

which gives the closed-loop transfer function

$$\frac{y_p}{r} = \frac{-2c_0^*(s+5)(s+1)}{[(s+1-\theta_1^*)(s-1)^2 + 2(s+5)(\theta_2^* + \theta_1^{*T}(s+1))]} = G_c(s)$$

Forcing $G_c(s) = \frac{3}{s+3}$, we have $c_0^* = -\frac{3}{2}$ and the matching equation becomes

$$\theta_1^*(s-1)^2 - 2(\theta_2^* + \theta_3^*(s+1))(s+5) = (s+1)(s-1)^2 - (s+1)(s+5)(s+3)$$

i.e.,

$$(\theta_1^* - 2\theta_3^*)s^2 + (-2\theta_1^* - 2\theta_2^* - 12\theta_3^*)s + \theta_1^* - 10(\theta_2^* + \theta_3^*) = -10s^2 - 24s - 14$$

Equating the powers of s we have

$$\theta_1^* - 2\theta_3^* = -10$$
$$2\theta_1^* + 2\theta_2^* + 12\theta_3^* = 24$$
$$\theta_1^* - 10\theta_2^* - 10\theta_3^* = -14$$

i.e.

$$\begin{bmatrix} 1 & 0 & -2 \\ 1 & 1 & 6 \\ 1 & -10 & -10 \end{bmatrix} \begin{bmatrix} \theta_1^* \\ \theta_2^* \\ \theta_3^* \end{bmatrix} = \begin{bmatrix} -10 \\ 24 \\ -14 \end{bmatrix}$$

Which gives

$$\begin{bmatrix} \theta_1^* \\ \theta_2^* \\ \theta_3^* \end{bmatrix} = \begin{bmatrix} -4 \\ -2 \\ 3 \end{bmatrix}$$

The control input is therefore given by

$$u_p = -4\frac{1}{s+1}u_p - 2\frac{1}{s+1}y_p + 3y_p - 1.5r$$

And implemented by

$$\dot{w}_1 = -w_1 + u_p$$

$$\dot{w}_2 = -w_2 + y_p$$

$$u_p = -4w_1 - 2w_2 + 3y_p - 1.5r$$

3.1.3 MRAC schemes for the system with unknown system parameters and relative degree n*=1

The design of the MRC to meet the objective defined in section 3.1 is as follows,

$$\dot{w}_1 = Fw_1 + gu_p \tag{3.19}$$

$$\dot{w}_2 = Fw_2 + gy_p \tag{3.20}$$

$$u_p = \theta^{*T} w \tag{3.21}$$

where $\theta^* = [\theta_1^{*T}, \theta_2^{*T}, \theta_3^*, C_0^*]^T$ are calculated by matching equations (3.17) and (3.18) to meet the MRC objective. However, for the plant with unknown plant parameters, because the parameters are unknown, controller parameter vector θ^* cannot be calculated and therefore cannot be implemented. An approach to deal with the unknown plant parameter case is using 'certainty equivalence' (CE).

$$\dot{w}_1 = Fw_1 + gu_p \tag{3.37}$$

$$\dot{w}_2 = Fw_2 + gy_p \tag{3.38}$$

$$u_p = \theta^T w \tag{3.39}$$

$\theta(t)$ is the estimate of θ^* at time t to be generated by an appropriate adaptive law. We derive such an adaptive law by following a similar procedure as described in section 3.1.1. We first obtain a composite state space representation of the plant and controller, i.e.,

$$\dot{Y}_c = A_0 Y_c + B_c u_p \tag{3.40}$$

$$y_p = C_c^T Y_c \tag{3.41}$$

$$u_p = \theta^T w \tag{3.42}$$

Where

$$Y_c = [x_p^T, w_1^T, w_2^T]^T \tag{3.43}$$

$$A_0 = \begin{bmatrix} A_p & 0 & 0 \\ 0 & F & 0 \\ gC_p^T & 0 & F \end{bmatrix} \qquad B_c = \begin{bmatrix} B_p \\ g \\ 0 \end{bmatrix} \tag{3.44}$$

$$C_c^T = [C_p^T \quad 0 \quad 0] \tag{3.45}$$

Then add and subtract the input $B_c \theta^{*T} w$ to obtain

$$\dot{Y}_c = A_0 Y_c + B_c \theta^{*T} w + B_c (\Delta u - \theta^{*T} w) \tag{3.46}$$

If we absorb the term $B_c \theta^{*T} w$ into the homogeneous part of the above equation, we end up with the representation

$$\dot{Y}_c = A_c Y_c + B_c c_0^* r + B_c (u_p - \theta^{*T} w) \tag{3.47}$$

$$y_p = C_c^T Y_c \tag{3.48}$$

where A_c is defined in (3.28). Equation (3.47) (3.48) is the same as (3.25) (3.26) in the known parameter case except for the additional input term $B_c(\Delta u - \theta^{*T} w)$ that depends on the choice of the input u_p. Let $e_1 = y_p - y_m$ and $e = Y_c - Y_m$ where Y_m is the state

of the non-minimal representation of the reference model defined in (3.33) (3.34). We obtain the error equation

$$\dot{e} = A_c e + B_c (u_p - \theta^{*T} w) \tag{3.49}$$

$$e_1 = C_c^T e \tag{3.50}$$

Because

$$C_c^T (sI - A_c)^{-1} B_c c_0^* = W_m(s) \tag{3.51}$$

We have

$$e_1 = W_m(s)\sigma^* (u_p - \theta^{*T} w) \tag{3.52}$$

Where

$$\sigma^* = \frac{1}{c_0^*} \tag{3.53}$$

Replace $u_p = \theta^T w$ and let $\tilde{\theta} = \theta(t) - \theta^*$, we rewrite (3.50) and (3.52) as

$$\dot{e} = A_c e + \bar{B}_c \rho^* \tilde{\theta}^T w \tag{3.54}$$

$$e_1 = C_c^T e \tag{3.55}$$

Where $$\bar{B}_c = B_c c_0^* \tag{3.56}$$

Or

$$e_1 = W_m(s)\sigma^* \tilde{\theta}^T w \tag{3.57}$$

Which relates the parameter error $\tilde{\theta}$ with the tracking error e_1. Because W_m is SPR (relative degree of W_m is equal to one) and A_c is stable, (3.54) and (3.55) are in the

appropriate form for applying the SPR-Lyapunov design approach [6]. We propose Lyapunov function

$$V(\tilde{\theta}, e) = \frac{1}{2}(e^T P_c e + \tilde{\theta}^T \Gamma^{-1} \tilde{\theta} \mid \rho^* \mid) \tag{5.58}$$

where $\Gamma^T = \Gamma > 0$ and $P_c^T = P_c > 0$ satisfy the algebraic equations

$$P_c A_c + A_c^T P_c = -qq^T - \nu_c L_c \tag{3.59}$$

$$P_c \bar{B}_c = C_c \tag{3.60}$$

where q is a vector; $L_c = L_c^T > 0$ and $\nu_c > 0$ is a small constant. The time derivative $\dot{V}$ of V along the solution of (3.54) and (3.55) is given by

$$\dot{V} = -\frac{e^T qq^T e}{2} - \frac{\nu_c}{2} e^T L_c e + e^T P_c \bar{B}_c \rho^* \tilde{\theta}^T w + \tilde{\theta}^T \Gamma^{-1} \dot{\tilde{\theta}} \mid \rho^* \mid \tag{3.61}$$

Because $e^T P_c \bar{B}_c = e^T C_c = e_1$ and $\rho^* = \mid \rho^* \mid \operatorname{sgn}(\rho^*)$, we can make $\dot{V} \le 0$ by choosing

$$\dot{\tilde{\theta}} = \dot{\theta} = -\Gamma e_1 w \operatorname{sgn}(\rho^*) \tag{3.62}$$

which leads to

$$\dot{V} = -\frac{e^T qq^T e}{2} - \frac{\nu_c}{2} e^T L_c e \le 0 \tag{3.63}$$

By equations (3.58) and (3.63), all signals in the closed-loop plant are bounded and the output tracking error e_1 converges to zero asymptotically with time given by

Theorem 3.1.

In the above MRAC schemes, the control parameter θ is estimated and generated directly by an adaptive law (3.61) and therefore it belongs to direct adaptive control.

3.1.4 MRAC schemes for the system with unknown system parameters and relative degree n*=2

In equation (3.57), since the relative degree of the plant $G_p(s)$ is equal to one, we can design the model reference $W_m(s)$ to be SPR and the control law $u_p = \theta^T w$ to obtain an error equation suitable for applying SPR-Lyapunove design method. When the relative degree $n^* = 2$, however, $W_m(s)$ can no longer be designed to be SPR and therefore the procedures of section 3.1.3 fail to apply in this case.

Thus, instead, we use the identity $(s + p_0)(s + p_0)^{-1} = 1$ to rewrite (3.50)(3.52) as

$$\dot{e} = A_c e + \bar{B}_c (s + p_0)\rho^* (u_f - \theta^{*T}\phi) \tag{3.64}$$

$$e_1 = C_c^T e \tag{3.65}$$

Or

$$e_1 = W_m(s)(s + p_0)\rho^* (u_f - \theta^{*T}\phi) \tag{3.66}$$

where

$$u_f = \frac{1}{s + p_0} u_p, \quad \phi = \frac{1}{s + p_0} w$$

And W_m, $p_0 > 0$, is chosen so that $W_m(s)(s+p_0)$ is SPR (the relative degree of $W_m(s)(s+p_0)$ is equal to one). Instead of the control law $u_p = \theta^T w$ in section 3.1.3 , if we choose u_p so that

$$u_f = \theta^T \phi \tag{3.67}$$

We obtain the error equation

$$\dot{e} = A_c e + \bar{B}_c (s+p_o)\rho^* \tilde{\theta}^T \phi \tag{3.68}$$

$$e_1 = C_c^T e \tag{3.69}$$

Or in the transfer form

$$e_1 = W_m(s)(s+p_0)\sigma^* \tilde{\theta}^T \phi \tag{3.70}$$

We transform the equation (3.68) (3.69) into the desired form by using

$$\bar{e} = e - \bar{B}_c \rho^* \theta^{*T} \phi$$

Then, we obtain

$$\dot{\bar{e}} = A_c \bar{e} + B_1 \rho^* \tilde{\theta}^T \phi \tag{3.71}$$

$$e_1 = C_c^T \bar{e} \tag{3.72}$$

Where

$$B_1 = A_c \bar{B}_c + \bar{B}_c p_0 \tag{3.73}$$

And $C_C^T \bar{B}_c = C_p^T B_p c_0^* = 0$ due to the relative degree $n^* = 2$. With (3.71) and (3.72), we can follow the same procedures in the case of $n^* = 1$ and develop an adaptive law for the

control estimate θ and get

$$\dot{\tilde{\theta}} = \dot{\theta} = -\Gamma e_1 \phi \operatorname{sgn}(\rho^*) \tag{3.74}$$

Come back to the control input u_p, it can be realized by

$$u_p = (s + p_o)u_f = (s + p_o)\theta^T \phi \tag{3.75}$$

It implies

$$u_p = \dot{\theta}^T \phi + \theta^T (s + p_0)\phi = \dot{\theta}^T \phi + \theta^T w \tag{3.76}$$

Because $\dot{\theta}$ can be made available by the adaptive law, the control law (3.76) can be implemented without using differentiators.

3.2 Adaptive Pole Placement Control

In section 3.1, we introduced the design of MRAC schemes for linear system with stable zeros. The assumption is rather restrictive in many applications. As we discussed in section 3.1, the minimum phase assumption is a consequence of the MRC objective that requires zeros cancellation to make closed-loop transfer function equal to that of reference model.

Another class of control schemes, Pole Placement Control (PPC) changes the poles of the plant but do not involve zero-pole cancellation and therefore are applicable to both minimum and non-minimum phase case. In the section, we will consider the Adaptive Pole Placement Control (APPC) which combines a PPC with a parameter estimator or an

adaptive law to control linear system with unknown system parameters.

3.2.1 Problem statement and assumption

This section is similar with section 3.1.1. We state the problem we desire to resolve and make assumption for the following control design.

Consider the linear plant

$$y_p = G_p(s)u_p \tag{3.77}$$

$$G_p = \frac{Z_p(s)}{R_p(s)} \tag{3.78}$$

The objectives of PPC is to choose the plant input u_p so that closed-loop poles are assigned to these of a given monic Hurwitz polynomial $A^*(s)$, which is referred to as the desired closed-loop characteristic polynomial and chosen based on performance requirements. Similar to MRAC, we have some assumptions as below:

(1) $G_p(s)$ Assumptions

P1. R_p is a monic whose degree n is known.

P2. R_p, Z_p are coprime and degree(Z_p)$< n$

P1 and ***P2*** allow R_p, Z_p to be non-Hurwitz in contrast to the MRC where Z_p is required to be Hurwitz. In general, by assigning the closed-loop poles to those of A^*, we

can guarantee closed-loop stability. We can also extend the PPC objective to include tracking, where output y_p is required to follow a certain class of reference signal y_m with a internal model $Q_m(s)$, satisfying (3.79) [10].

$$Q_m(s)y_m = 0 \tag{3.79}$$

$Q_m(s)$ is a monic polynomial of degree q with non-repeated roots on the jw-axis and satisfy (P3)

P3. $Q_m(s)$, Z_p are coprime.

For example, if $y_m = 2 + \sin(2t)$, then the internal model of y_m, $Q_m(s) = s(s^2 + 4)$ and therefore, according to **P3**, Z_p should have s or $s^2 + 4$ as a factor.

3.2.2 PPC schemes for the system with known parameters

We first consider the control law (3.80) as Figure 3.3

$$Q_m(s)L(s)u_p = -P(s)y_p + M(s)y_m \tag{3.80}$$

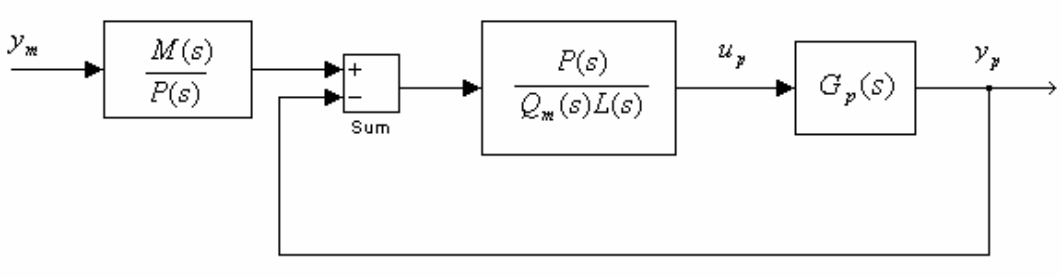

Fig. 3.3 Pole placement control

where $P(s), L(s), M(s)$ are polynomials of degree $q+n-1, n-1, q+n-1$ respectively and can be designed so that characteristic equations of closed-loop plant equals to $A^*(s)$.

Applying (3.77) to (3.80), we obtain closed-loop plant equation

$$y_p = \frac{Z_p M}{LQ_m R_p + PZ_p} y_m \tag{3.81}$$

whose characteristic equation

$$LQ_m R_p + PZ_p = 0 \tag{3.82}$$

has a order $2n+q-1$. Therefore, the objective now is choose P, L such that

$$LQ_m R_p + PZ_p = A^* \tag{3.83}$$

is satisfied for a given monic Hurwitz polynomials $A^*(s)$ of degree $2n+q-1$. Since P2 and P3 guarantee that $Q_m R_p, Z_p$ are coprime, we have a unique solution P, L satisfying (3.83). The solution for the coefficient of $P(s), L(s)$ may be obtained by resolving the algebraic equation (3.84).

$$S_l \beta_l = \alpha_l^* \tag{3.84}$$

where S_l is the Sylvester matrix (See Theorem 3.2) of $Q_m R_p$, Z_p of dimensional $2(n+q)\times 2(n+q)$

$$\beta_l = [l_q^T, p^T]^T, \quad \alpha_l^* = [0 \quad ... \quad 0 \quad 1 \quad \alpha^{*T}]^T, \qquad \in \Re^{2(n+q)}$$

$$l_q = [0 \quad ... \quad 0 \quad 1 \quad l^T]^T \qquad \in \Re^{n+q}$$

$$l = [l_{n-2} \quad l_{n-3} \quad ... \quad l_1 \quad l_0]^T \quad \in \Re^{n-1}$$

$$p = [p_{n+q-1} \quad p_{n+q-2} \quad ... \quad p_1 \quad p_0]^T \quad \in \Re^{n+q}$$

$$\alpha^* = [a^*_{2n+q-2} \quad a^*_{2n+q-3} \quad ... \quad a^*_1 \quad a^*_0]^T \quad \in \Re^{2n+q-1}$$

l_i , p_i , a_i^* are the coefficients of

$$L(s) = s^{n-1} + l_{n-2}s^{n-2} + ... + l_1 s + l_0 = s^{n-1} + l^T \alpha_{n-2}(s)$$

$$P(s) = p_{n+q-1}s^{n-1} + p_{n+q-2}s^{n-2} + ... + p_1 s + p_0 = p^T \alpha_{n+q-1}(s)$$

$$A^*(s) = s^{2n+q-1} + a^*_{2n+q-2}s^{2n+q-2} + ... + a^*_1 s + a^*_0 = s^{2n+q-1} + \alpha^{*T} \alpha_{2n+q-2}(s)$$

The coprime of $Q_m R_p$, Z_p guarantee that S_l is nonsingular; therefore, the coefficients of $P(s), L(s)$ may be computed from

$$\beta_l = S_l^{-1} \alpha_l^* \tag{3.85}$$

By (3.83), the closed-loop plant is describe by

$$y_p = \frac{Z_p M}{A^*} y_m \tag{3.86}$$

Similarly, by (3.77),(3.80)

$$u_p = \frac{R_p M}{A^*} y_m \tag{3.87}$$

Because $\frac{Z_p M}{A^*}$, $\frac{R_p M}{A^*}$ are proper with stable poles, it follows that u_p and y_p are bounded if bounded u_p for any polynomial $M(s)$ of degree $q+n-1$.Therefore, the pole placement objectives is achieved by the control law (3.80) without any additional restriction of $M(s)$ and $Q_m(s)$ .Choose $M(s) = P(s)$, the control law become

$$Q_m(s)L(s)u_p = -P(s)(y_p - y_m) \tag{3.88}$$

Then, the diagram is as in Fig. 3.4.

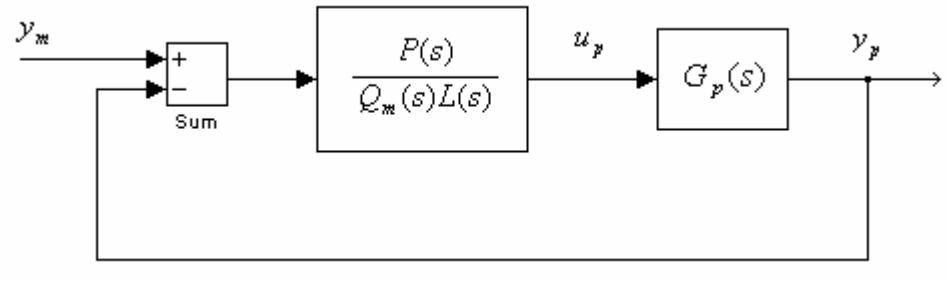

Figure 3.4 Block diagram of pole placement control

Because $L(s)$ is not necessary Hurwitz, the alternative realization of (3.88) is obtained by rewriting (3.88) as

$$u_p = \frac{\Lambda - LQ_m}{\Lambda} u_p - \frac{P}{\Lambda}(y_p - y_m) \tag{3.89}$$

where Λ is any monic Hurwitz polynomial of degree $q+n-1$. The control law is implemented as Fig. 3.5. It uses $2(q+n-1)$ integrators to realize the proper stable transfer function $\frac{\Lambda - LQ_m}{\Lambda}, \frac{P}{\Lambda}$.

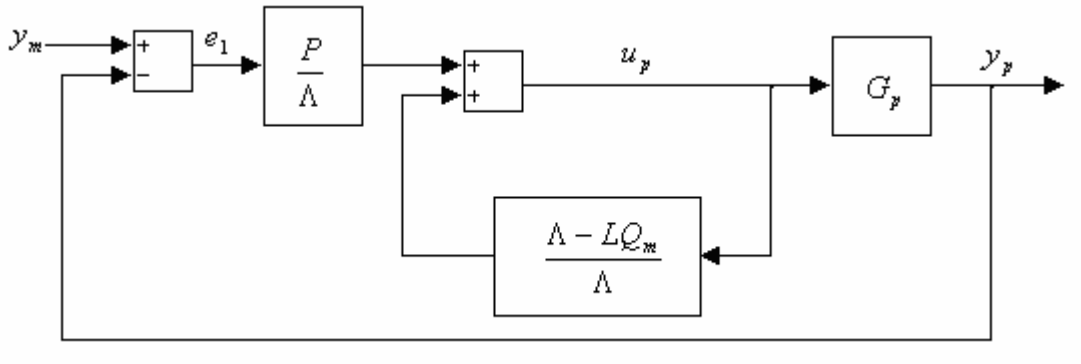

Fig. 3.5 Implementation of pole placement control

(1) Example 3.2.2

Consider the plant

$$y_p = \frac{2}{s-1} u_p$$

The control objective is to choose u_p such that the poles of the closed-loop are placed at the roots of $A^* = (s+1)^2$ and y_p tracks the constant reference signal $y_m = 1$. Clearly that internal model of y_m is $Q_m(s) = s$, i.e. $q = 1$. Because $n = 1$, the polynomial $P(s), L(s)$ are of the form

$$P(s) = 1, \quad L(s) = p_1 s + p_0$$

Choosing $\Lambda(s) = s + 3$, p_1, p_0 are calculated by solving

$$s(s-1) + (p_1 s + p_0)2 = (s+1)^2$$

Equating the coefficients of power s, we obtain

$$p_1 = \frac{3}{2}, \quad p_2 = \frac{1}{2}$$

It may be also written in the form of the algebraic equation (3.2.9)where the Sylvester matrix of $s(s-2)$, 2

$$S_l = \begin{bmatrix} 1 & 0 & 0 & 0 \\ -1 & 1 & 0 & 0 \\ 0 & -1 & 2 & 0 \\ 0 & 0 & 0 & 2 \end{bmatrix}$$

$$\beta_l = \begin{bmatrix} 0 \\ 1 \\ p_1 \\ p_2 \end{bmatrix} \qquad \alpha_l^* = \begin{bmatrix} 0 \\ 1 \\ 2 \\ 1 \end{bmatrix}$$

Therefore, the PPC law is given by

$$u_p = \frac{3}{s+3}u_p - \frac{3s+1}{2(s+3)}(y_p - y_m)$$

A state-space realization of the control law is given by

$$\dot{\phi}_1 = -3\phi_1 + u_p$$

$$\dot{\phi}_2 = -3\phi_2 + e_1$$

$$u_p = 3\phi_1 + 4\phi_2 - \frac{3}{2}e_1$$

Where $e_1 = y_p - y_m = y_p - 1$

3.2.3 Adaptive pole placement control schemes for unknown parameters

Let's now consider (3.78) when the coefficient of $R_p(s), Z_p(s)$ are unknown. Similarly to MRAC, APPC scheme is formed by combining the control law (3.2.13) with an adaptive law based on the parametric model. The adaptive law generate on-line estimates θ_a, θ_b of the coefficients θ_a^* of $R_p(s) = s^n + \theta_a^{*T}\alpha_{n-1}(s)$ and θ_b^* of $Z_p(s) = \theta_b^{*T}\alpha_{n-1}(s)$, respectively, to form the estimated plant polynomials

$$\hat{R}_p(s,t) = s^n + \theta_a^T\alpha_{n-1}(s), \quad \hat{Z}_p(s,t) = \theta_b^T\alpha_{n-1}(s)$$

The estimated polynomials are used to compute the estimated controller polynomials

$\hat{L}(s,t)$, $\hat{R}(s,t)$ by solving the Diophantine equations (3.91) or (3.90)in time

$$\hat{L}Q_m\hat{R}_p + \hat{P}\hat{Z}_p = A^* \tag{3.90}$$

$$\hat{S}_l\hat{\beta}_l = \alpha_l^* \tag{3.91}$$

The control law in the unknown parameter case is then formed as

$$u_p = \frac{\Lambda - \hat{L}Q_m}{\Lambda}u_p - \frac{\hat{P}}{\Lambda}(y_p - y_m) \tag{3.92}$$

We first rewrite (3.77) as a linear parametric model, i.e.

$$R_p(s)y_p = Z_p(s)u_p$$

$$[s^n + \theta_a^{*T}\alpha_{n-1}(s)]y_p = [\theta_b^{*T}\alpha_{n-1}(s)]u_p \tag{3.93}$$

Filtering (3.92) with $\frac{1}{\Lambda_p(s)}$, where $\Lambda_p(s) = s^n + \lambda_{n-1}s^{n-1} + ... + \lambda_1 s + \lambda_0$ is a monic Hurwitz polynomials, we obtain

$$z = \theta_p^{*T}\phi \tag{3.94}$$

where

$$z = \frac{s^n}{\Lambda_p(s)}y_p, \quad \theta_p^* = [\theta_b^{*T} \quad \theta_a^{*T}]^T, \quad \phi = [\frac{\alpha_{n-1}^T(s)}{\Lambda_p(s)}u_p \quad -\frac{\alpha_{n-1}^T(s)}{\Lambda_p(s)}y_p]^T \tag{3.95}$$

Similarly, instead of eq. (3.93)

$$y_p = \theta_\lambda^{*T}\phi \tag{3.96}$$

Where $\theta_{\lambda}^{*} = [\theta_b^{*T} \quad (\theta_a^{*} - \lambda_p)^T]^T$ and $\lambda_p = [\lambda_{n-1} \quad \lambda_{n-2} \quad ... \quad \lambda_0]^T$ is the coefficients of $\Lambda_p(s) - s^n$. After getting the linear parametric model of y_p and u_p, on-line parameter estimator of θ_a, θ_b could be derived from several adaptive laws such as SPR-Lyapunov approaches, Gradient algorithm, Least-square algorithm and etc. In the thesis, our APPC schemes is based on Gradient algorithm approaches as below:

$$\dot{\theta}_p = \Gamma \varepsilon \phi, \qquad \Gamma = \Gamma^T > 0 \tag{3.97}$$

Where

$$\varepsilon = \frac{(z - \theta_p^T \phi)}{m^2} \quad , m = 1 + \phi^T \phi \tag{3.98}$$

ε, z is defined as (3.95).

Then all signals in the closed-loop APPC schemes of the thesis are uniformly bounded and the tracking error $e_1 = y_p - y_m$ converges to zero asymptotically. See the detail proof in [10].

In the above APPC schemes, the plant parameters θ_p is estimated on-line by the adaptive law (3.96) and then controller parameters $\hat{L}(s,t)$, $\hat{R}(s,t)$ are compute by solving algebraic equation (3.2.90) or (3.2.91) but not directly estimated by the adaptive laws such as equation (3.62). Such an approach is so-called indirect adaptive control.

3.3 Theorem and Definition

Theorem 3.1

Suppose that there exist a positive definite function $V(x,t):\Re^{+}\times B(r)\mapsto\Re$, for some r>0 with continuous first order partial derivatives with respective to x, t and $V(x=0,t)=0$ for t>0. Then the following statements are hold:

(i) If V' $\leqq$ 0, then $x_e = 0$ is stable.

(ii) If V is decrescent and V' $\leqq$ 0, then $x_e = 0$ is uniformly stable.

(iii) If V is decrescent and V' $<$ 0, then $x_e = 0$ is uniformly asymptotically stable.

Theorem 3.2

For an n-order system:

$$\dot{x} = A\dot{x} + Bu$$

Let (A, B) be a controller pair. If input u is sufficient rich of order n+1, the estimate $\hat{A}$ and $\hat{B}$ generated by

$$\dot{\hat{x}} = \hat{A}\hat{x} + \hat{B}u$$

$$\dot{\hat{A}} = \gamma_1\varepsilon_1 x^T, \quad \dot{\hat{B}} = \gamma_2\varepsilon_1 u^T$$

$$\varepsilon_1 = x - \hat{x}$$

converges exponentially fast to the unknown parameter A and B, respectively.

Definition 3.1

Input u is sufficient rich of order n+1 if and only if input u contains at least (n+1)/2 different frequency components [6].

Theorem 3.3

Two polynomials $a(s)$ and $b(s)$ are coprime if and only if their Sylvester's matrix S_l is nonsingular, where S_l is defined to be the following $2n \times 2n$ matrix:

$$a(s) = a_n s^n + a_{n-1} s^{n-1} + ... a_1 s + a_0$$

$$b(s) = b_n s^n + b_{n-1} s^{n-1} + ... b_1 s + b_0$$

$$S_l \equiv \begin{bmatrix}
a_n & 0 & 0 & ... & 0 & 0 & b_n & 0 & 0 & ... & 0 & 0 \\
a_{n-1} & a_n & 0 & ... & 0 & 0 & b_{n-1} & b_n & 0 & ... & 0 & 0 \\
a_{n-2} & a_{n-1} & a_n & ... & 0 & 0 & b_{n-2} & b_{n-1} & b_n & ... & 0 & 0 \\
\vdots & \vdots & \vdots & ... & \vdots & \vdots & \vdots & \vdots & \vdots & ... & \vdots & \vdots \\
a_2 & \vdots & \vdots & ... & a_n & 0 & b_2 & \vdots & \vdots & ... & b_n & 0 \\
a_1 & a_2 & \vdots & ... & a_{n-1} & a_n & b_1 & b_2 & \vdots & ... & b_{n-1} & b_n \\
a_0 & a_1 & a_2 & ... & a_{n-2} & a_{n-1} & b_0 & b_1 & b_2 & ... & b_{n-2} & b_{n-1} \\
0 & a_0 & a_1 & ... & a_{n-3} & a_{n-2} & 0 & b_0 & b_1 & ... & b_{n-2} & b_{n-2} \\
0 & 0 & a_0 & ... & \vdots & a_{n-3} & 0 & 0 & b_0 & ... & \vdots & b_{n-3} \\
\vdots & \vdots & \vdots & ... & \vdots & \vdots & \vdots & \vdots & \vdots & ... & \vdots & \vdots \\
0 & 0 & 0 & ... & a_0 & a_1 & 0 & 0 & 0 & ... & b_0 & b_1 \\
0 & 0 & 0 & ... & 0 & a_0 & 0 & 0 & 0 & ... & 0 & b_0
\end{bmatrix}$$

CHAPTER IV

ADAPTIVE CONTROL FOR NONLINEAR DAE SYSTEM

We will use the adaptive controller presented in the previous section in order to control our nonlinear power system. As we mentioned in the section <2>, the feedback control law $\Delta u = h(\Delta z, \theta)$ is implemented by Δx and θ. The controller parameter θ could be estimated and generated directly or indirectly by MRAC or APPC schemes while $\Delta x = x - x_{ei}$ should be calculated by x_{ei}. However, the equilibrium x_{ei} would change as the operating condition p_i changes and therefore is not available. We would propose a dynamic mechanism to track the nonlinear system's equilibrium value or force the equilibrium value of the measurable output unchanged by some control law. Power system examples are demonstrated to show our approaches improving the structure stability of power system and therefore increasing the loadability.

4.1 Equilibrium Tracking

4.1.1 Dynamic equilibrium tracking

We could refer x_{ei} as an uncertainty parameter in the control law and apply a certainty equivalence adaptive control, i.e. instead of using the true value of x_{ei}, we use an estimate $\hat{x}_{ei}$. The resulting controller is describe by

$$\Delta u = h(\Delta z, \theta) = h(x - \hat{x}_{ei}, \theta) \tag{4.1}$$

$$\dot{\hat{x}}_{ei} = \beta(x - \hat{x}_{ei}) \tag{4.2}$$

With $\beta > 0$. If we consider x as a constant, because of $\beta > 0$ (negative eigenvalue), the estimate $\hat{x}_{ei}$ will finally converge to x. If the system is stable, the trajectories would be around the equilibrium manifold, $\hat{x}_{ei}$ could be considered equal to x. If the system, however, becomes unstable, x will diverge from its true equilibrium value x_{ei}. Therefore, we need this tracking mechanism to work just as a low-pass filter to get the estimated equilibrium value of $\hat{x}_{ei}$. See Fig. 4.1.

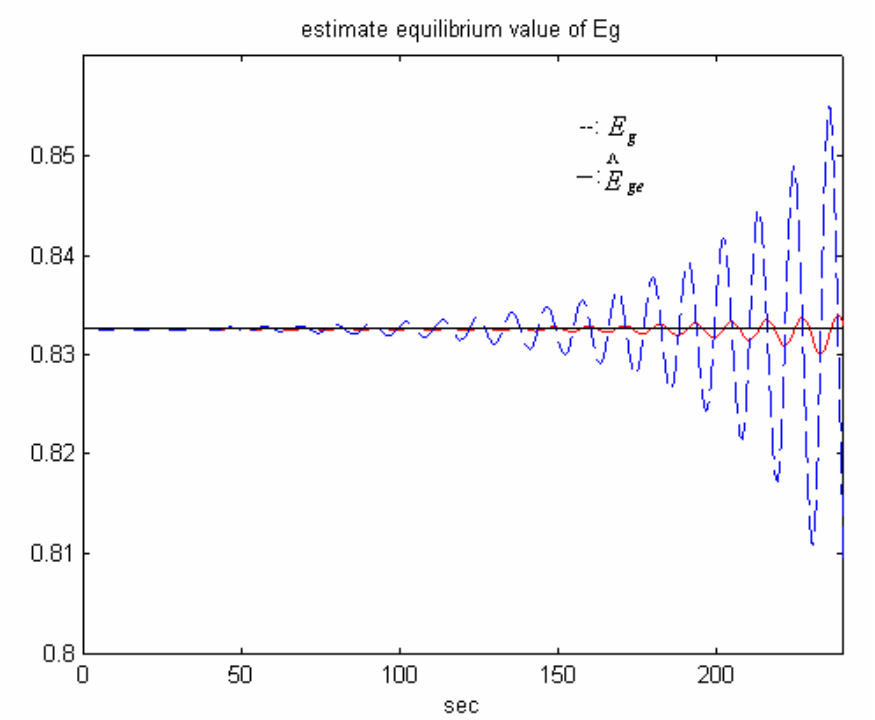

Fig. 4.1 Time response of estimated equilibrium value for unstable condition

4.1.2 Measurement of the changing dynamic state x

As we mention in the previous section, the equilibrium point for a given operation condition p_i satisfying,

$$0 = f(x_{ei}, y_{ei}, p_i) \tag{4.3}$$
$$0 = g(x_{ei}, y_{ei}, p_i) \tag{4.4}$$

Since the system dynamic is continuous, around the equilibrium (x_{ei}, y_{ei}), the changing rate of the state x would be close to zeros, i.e.,

$$\dot{x} \cong 0 \tag{4.5}$$

Therefore, if we sense $\dot{x} \cong 0$, the dynamic states (x, y) is very near its equilibrium (x_{ei}, y_{ei}), then we can update $\hat{x}_{ei}$ by the x when $\dot{x} \cong 0$.

4.1.3 Apply control laws to force steady-state value of output unchanged

In most control case, not all states of the system is available as a feedback control, it may be that only a single output could be as feedback control signal. If we could achieve regulation of the output by some control law, then the equilibrium value of output y_p would be equal to the set-point value and would not change with operation condition p_i.

(1) Example 4.1 Tracking the equilibrium

We take two two-bus power systems as examples: one is the system with P controller and the other is with PI controller to explain the above approaches to estimate x_{ei} .

P Controller

We have a DAE equation of the simplified model:

$$\dot{E}' = \frac{1}{T_{d0}'}\left[-\frac{x+x_d}{x'}E' + \frac{x_d - x_d'}{x'}\frac{E^2 + x'Q}{E'} + E_{fd}\right] \tag{4.6}$$

$$\dot{E}_{fd} = \frac{1}{T}\left[-(E_{fd} - E_{fd0}) - K(E_g - E_r)\right] \tag{4.7}$$

$$0 = E'^2E^2 - (x'P)^2 - (x'Q + E^2)^2 \tag{4.8}$$

The system parameter $p=\{P, Q\}$ is changing or uncertainly power load and $E_g = \frac{1}{E}\sqrt{(xP)^2 + (xQ + E^2)^2}$ is generator bus voltage only measurable for feedback control. It is obvious that the steady-state value of E_g , or equilibrium value of E_g , E_{ge} is decreasing as load P increasing, increasing as P decreasing. Therefore, we must implement a dynamic tracking of E_{ge} for our control (4.9).

$$\Delta u = h(\Delta E_g, \theta) = h(E_g, \hat{E}_{ge}, \theta) \tag{4.9}$$

where θ is controller parameter generated by MRAC or APPC and equilibrium of $\hat{E}_{ge}$

is generated by

$$\dot{\hat{E}}_{ge} = \beta(E_g - \hat{E}_{ge}) \tag{4.10}$$

where $\beta > 0$.

PI Controller

If we add an extra dynamic input ΔE_{fd0} (it can be referred to as a PI controller)

$$\dot{E}' = \frac{1}{T_{d0}'}\left[-\frac{x + x_d}{x'}E' + \frac{x_d - x_d'}{x'}\frac{E^2 + x'Q}{E'} + E_{fd}\right] \tag{4.11}$$

$$\dot{E}_{fd} = \frac{1}{T}\left[-(E_{fd} - E_{fd0} - \Delta E_{fd0}) - K(E_g - E_r)\right] \tag{4.12}$$

$$\dot{\Delta E}_{fd} = \gamma(E_r - E_g) \tag{4.13}$$

$$0 = E'^2E^2 - (x'P)^2 - (x'Q + E^2)^2 \tag{4.14}$$

From (4.13), we know $E_{ge} = E_r = 1$, no matter the load $\{P, Q\}$ change. Therefore, we could implement $\Delta u = h(E_g - 1, \theta)$ directly without any equilibrium tracking. However, for the system (4.11)-(4.14) is three-order and requires more parameter estimators than the system (4.6)-(4.8).

4.2 Examples of Applying an Auxiliary MRAC

4.2.1. First-order example

Let us take a first-order example to illustrate our application.

$$\dot{x} = -yx + 2p \tag{4.15}$$

$$0 = -y^2 + y\sqrt{1-x^2} - p \tag{4.16}$$

$$x \in X \subset \Re,\ y \in Y \subset \Re,\ p \in P \subset \Re$$

where p is a positive scalar parameter. For each p_i, we have one interested equilibrium point (x_e, y_e). By Taylor's expansions we get a linear reduced model:

$$\Delta \dot{x} = \lambda_i \Delta x \tag{4.17}$$

where λ_i is RJM which depends on p_i, if λ_i is positive, the equilibrium point (x_e, y_e) is unstable and therefore we must design a feedback control $\Delta u = -k\Delta x$ to make the close-loop system (4.18) become stable.

$$\Delta \dot{x} = \lambda_i \Delta x - k\Delta x = (\lambda_i - k)\Delta x \tag{4.18}$$

Since k must be greater than λ_i to obtain stable closed-loop system, we could apply MRAC to estimate λ_i. Figure 4.2 is the phase portrait at $p = 0.14$, in the case, we assume that an interested equilibrium point $(x_e = 0.6559, y_e = 0.4269)$ is exactly known but λ_i is unknown and apply MRAC.

$$\Delta \dot{x} = \lambda_i \Delta x - k\Delta x \tag{4.19}$$

$$\dot{k} = \Delta x^2 \tag{4.20}$$

where

$$\Delta x = x - 0.6559$$

In the case, we set the reference signal $x_m \equiv 0$. Δx would trace and follow x_m. That is, Δx is forced to converge to zeros. From Fig. 4.2 and equation (4.19) (4.20), we know that the system (4.15) (4.16) has infinite equilibrium points at $\Delta x = 0$. For $k > 2.0332$, the equilibrium is stable while for $k < 2.0332$ the equilibrium is unstable. If the initial condition $\Delta x(0) \neq 0$, the adaptive feedback control coefficient k would continues to increase until $\Delta x = 0$ since $\dot{k} = \Delta x^2 \geq 0$.

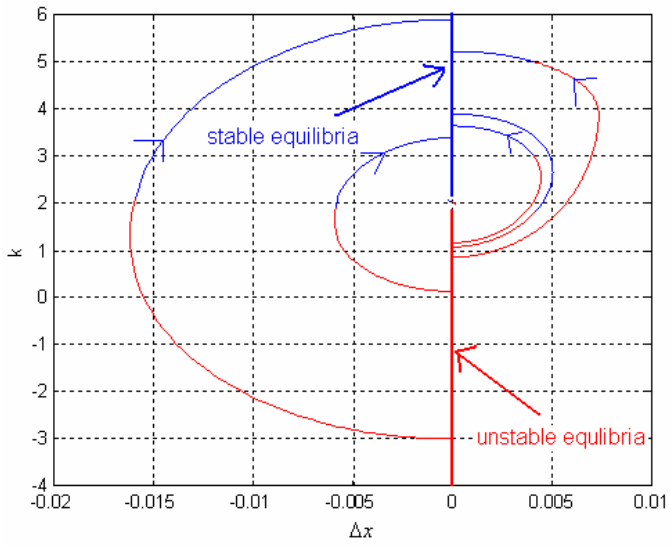

Fig. 4.2 Phase portrait of adaptive control for first-order example

4.2.2 Second-order example

Consider the 2-bus power system example again,

$$\dot{E}' = \frac{1}{T_{d0}'}\left[-\frac{x + x_d}{x'} E' + \frac{x_d - x_d'}{x'} \frac{E^2 + x'Q}{E'} + E_{fd} \right] \tag{4.21}$$

$$\dot{E}_{fd} = \frac{1}{T}\left[-(E_{fd} - E_{fd0}) - K\left(\frac{1}{E}\sqrt{(xP)^2 + (xQ + E^2)^2} - E_r\right) \right] \tag{4.22}$$

$$0 = E'^2 E^2 - (x'P)^2 - (x'Q + E^2)^2 \tag{4.23}$$

With coefficients

$$T_{d0}' = 5,\ T = 1.5,\ E_{fd0} = 1.6,\ x_d = 1.2,\ x_d' = 0.2,$$
$$x = 0.1,\ x' = x + x_d',\ Q = 0.5P,\ E_r = 1.0$$

We apply the MRAC schemes we introduced in the section <3> in order to improve the structural stability of the power system.

In the two-bus power system example, the relative degree of the linearized model is $n^* = 2$, therefore, it has no zeros and therefore is minimum phase and applicable for MRAC.

<**Step 1**> Propose a dynamic mechanism (4.2.10) to track equilibrium E_{ge}.

$$\dot{\hat{E}}_{ge} = \beta(E_g - \hat{E}_{ge}) \tag{4.24}$$

In our case, we set $\beta = 0.1$.

<**Step 2**> Propose MRAC

We choose model reference which relative degree is two as (4.2.11)

$$W_m(s) = \frac{1}{s^2 + s + 1} \tag{4.25}$$

Therefore, the desired trajectory y_m is generated by

$$\begin{aligned} \dot{w}_0 &= \begin{bmatrix} -1 & -1 \\ 1 & 0 \end{bmatrix} w_0 + \begin{bmatrix} 1 \\ 0 \end{bmatrix} r \\ y_m &= \begin{bmatrix} 0 & 1 \end{bmatrix} w_0 \end{aligned} \tag{4.26}$$

where r is the reference input of reference model.

Let feedback control law Δu_p as (4.2.13)

$$\Delta u_p = \dot{\theta}^T \phi + \theta^T w \tag{4.27}$$

Where w is generated by

$$\dot{w}_1 = F w_1 + g \Delta u_p \tag{4.28}$$

$$\dot{w}_2 = F w_2 + g (E_g - \hat{E}_{ge}) \tag{4.29}$$

And ϕ is generated by

$$\dot{\phi} = -p_0 \phi + w \tag{4.30}$$

where $w = [w_1^T, w_2^T, (E_g - \hat{E}_{ge}), r]^T$

Choose $F = \begin{bmatrix} -2 \end{bmatrix}$, $g = \begin{bmatrix} 1 \end{bmatrix}$, $p_o = 1$

The controller parameter θ is directly generated by the adaptive law

$$\dot{\theta} = \Gamma e_1 \phi \operatorname{sgn}(k_p / k_m) \tag{4.31}$$

where $sign(k_p / k_m) = 1$

Choose $\Gamma = 200$ and $e_1 = (E_g - \hat{E}_{ge}) - y_m$

By equations (4.21)-(4.31), we have an original DAE system with an auxiliary adaptive control. Fig. 4.3 shows our diagram for the original DAE with the additional adaptive control.

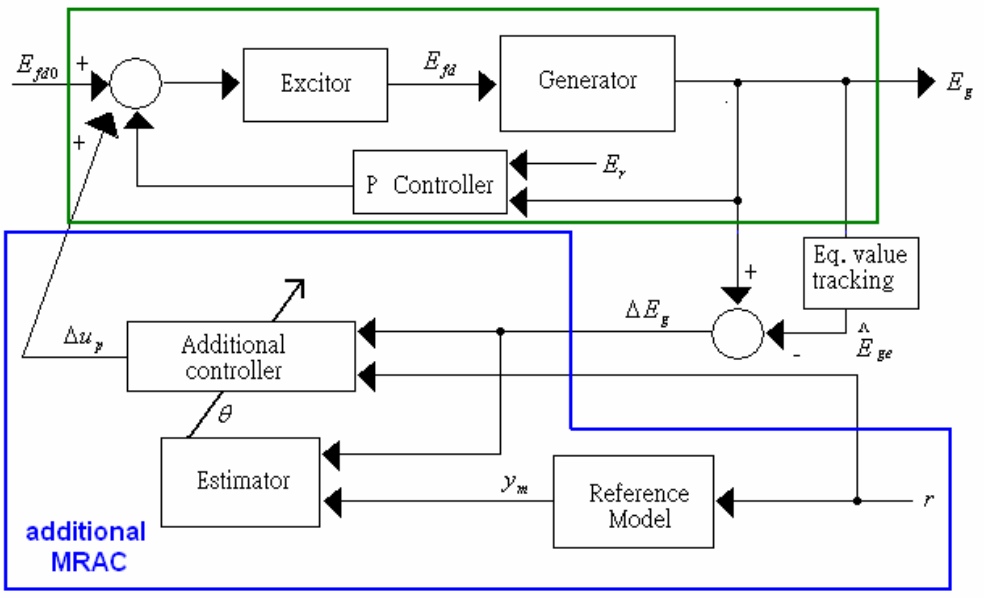

Fig. 4.3 Block diagram of the two-bus system with MRAC

(1) Simulation results for case of the system without P control ($K = 0$)

Without MRAC

Let us see the time response of the generate bus voltage E_g as P slowly increasing without the auxiliary MRAC, i.e., set $\Delta u_p \equiv 0$. Figure 4.4 shows that the voltage will collapse after P over SNB.

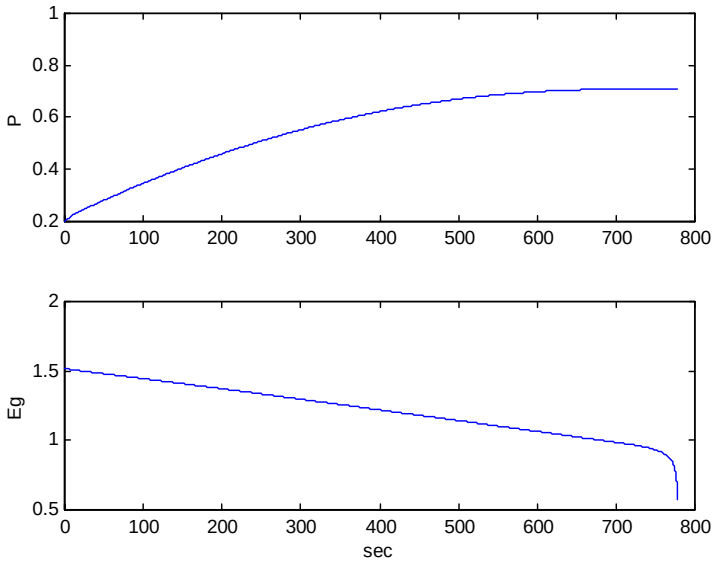

Fig. 4.4 Time response as load increases for neither P control nor MRAC case

Then, since the trajectories move along the equilibrium manifold, we draw its PV curve as in Fig. 4.5,

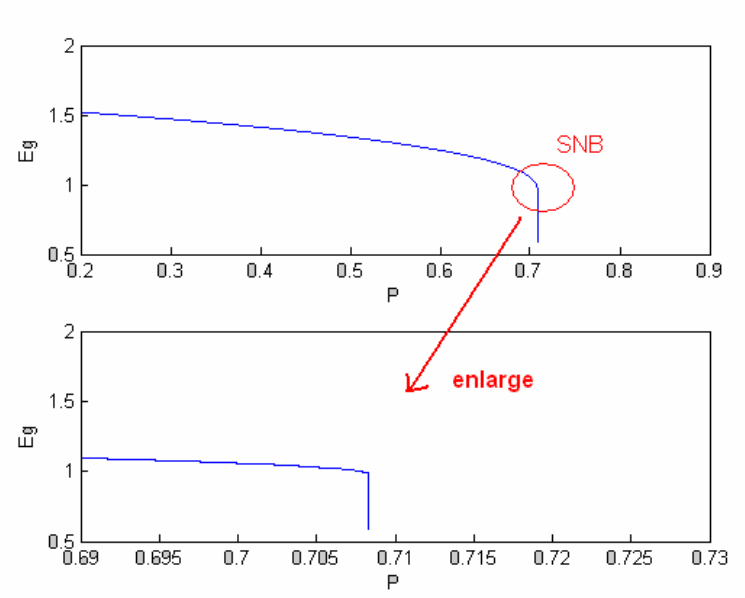

Fig. 4.5 PV curve for neither P control nor MRAC case

With MRAC

We observe the time response of E_g with our auxiliary MRAC in Fig. 4.6 where reference input is set to $r \equiv 0$.

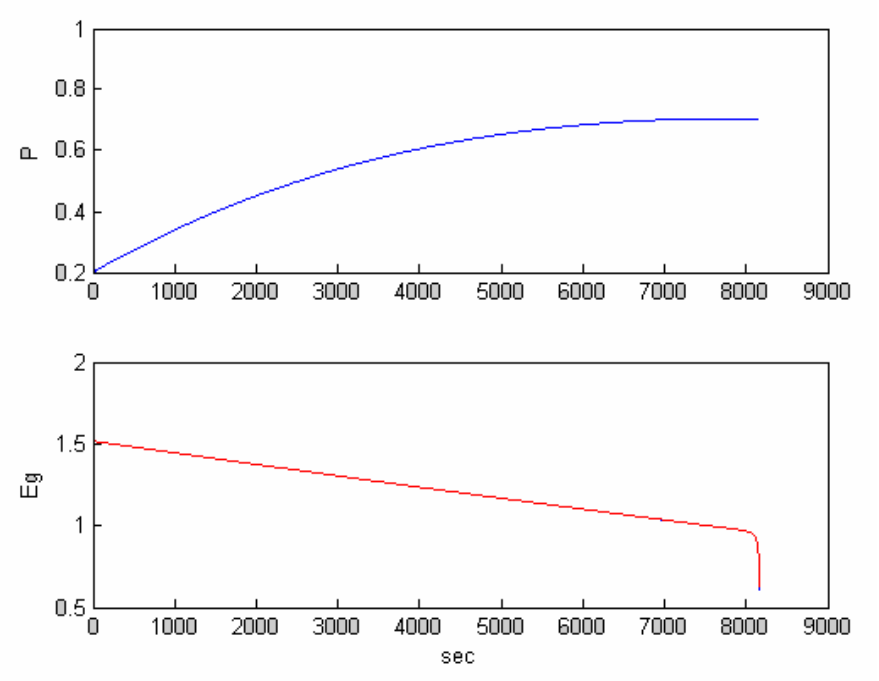

Fig. 4.6 Time response for the system without P control with MRAC case

Similarly, we draw its PV curve as Fig. 4.7 We also compare PV curve of the case with/without additional MRAC in the Fig. 4.8.

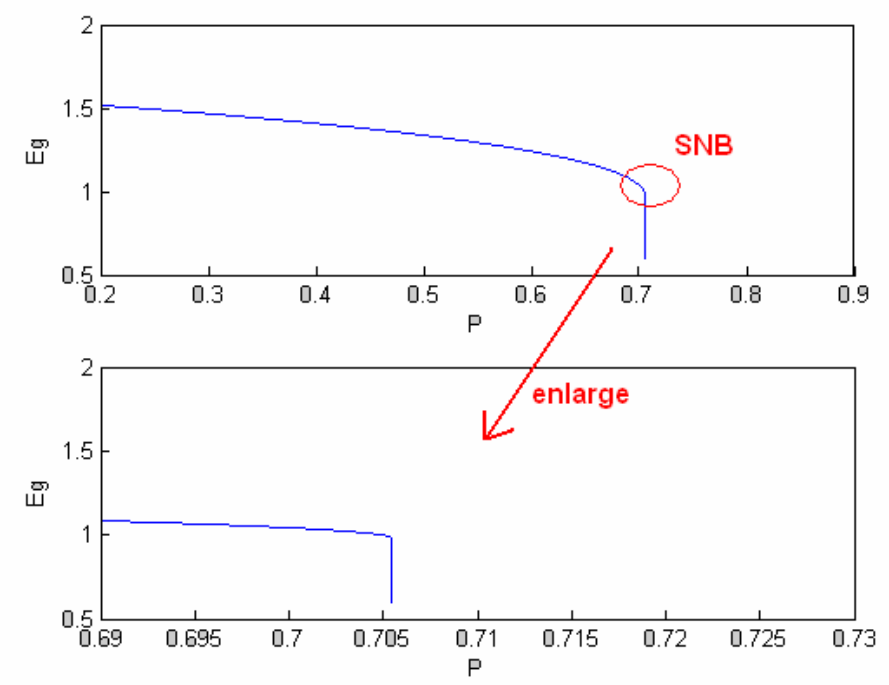

Fig. 4.7 PV curve for the case without P control with MRAC

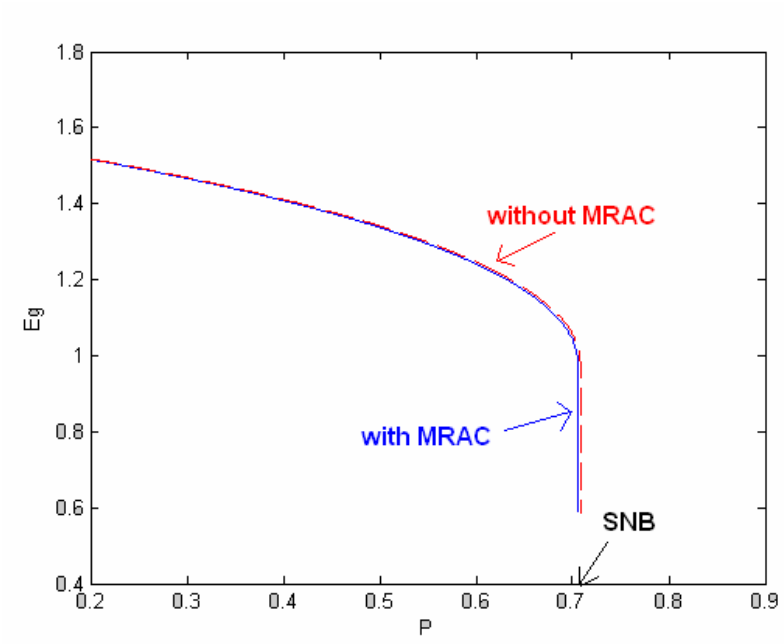

Fig. 4.8 Comparison of MRAC for the case without P control

As we mention at first, the additional MRAC does not change the original PV curve but stabilize the unstable equilibrium along the original PV curve. It can be confirmed by the simulation results. In such a case, the MRAC applied to nonlinear system does not guarantee the stability [17][18][19] since the unmodeled dynamics (it is often due to nonlinearity) near SNB may become more dominant.

(2) Simulation results for case of the system with P control ($K = 3.2$)

Without MRAC

In the same way, we observe the time response for load slowly increasing and draw its PV curve as in Fig. 4.9. From the figure, we know as the power load is increased by HB, the trajectories oscillate and diverge.

With MRAC

Similarly, as power load gradually increasing, we first observe its time response for generator bus voltage and its estimated equilibrium value (Fig. 4.10) and the feedback signal and the estimated control parameter (Fig. 4.11).

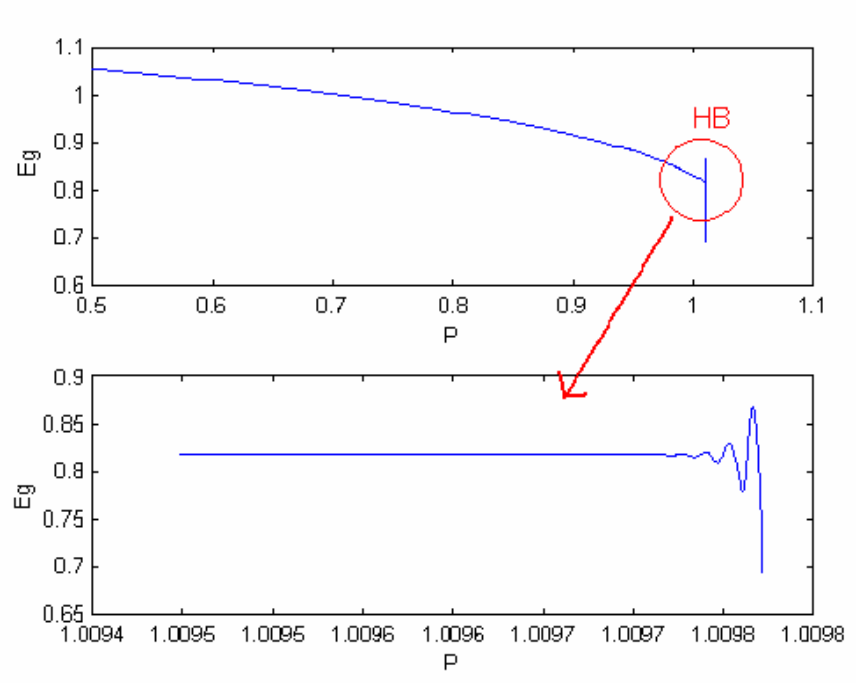

Fig. 4.9 PV curve for the case with P control without MRAC

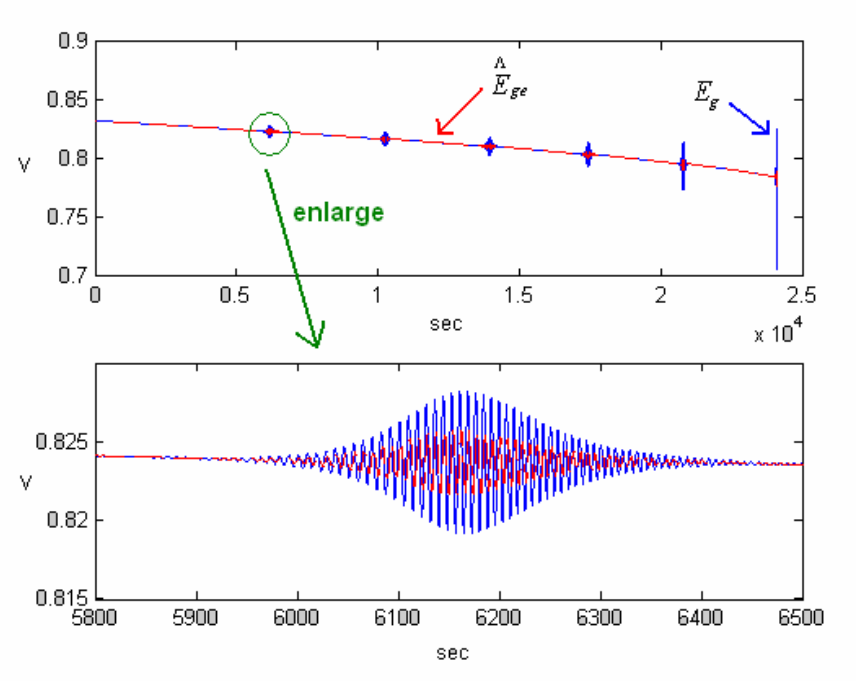

Fig. 4.10 Time response of generator bus voltage and its estimated equilibrium as load increases for the case with P control and MRAC

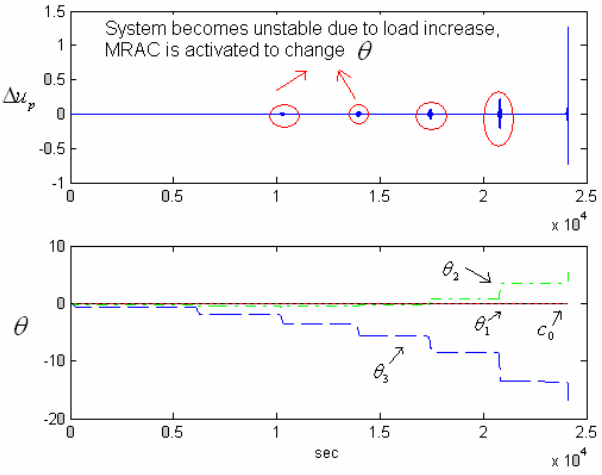

Fig. 4.11 Feedback signal and estimated control parameter for P control with MRAC

Then, we draw the PV curve as un Fig. 4.12. We see that as power load increasing to over HB, the system become unstable and trajectories start to diverge. The MRAC could detect its divergence and is activated to change control parameter and stabilize the unstable equilibrium and finally the trajectories converge to its equilibrium again.

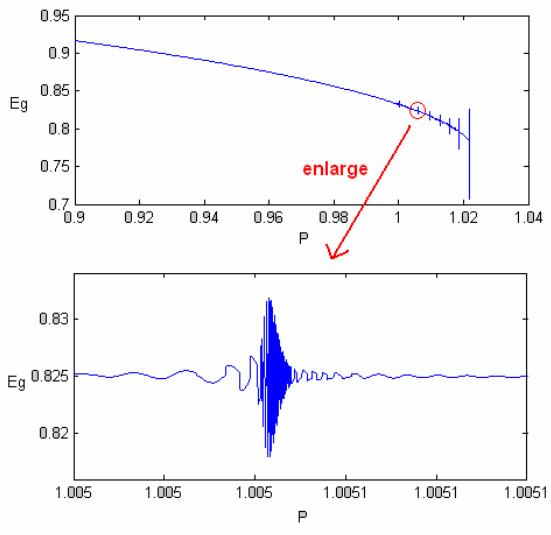

Fig. 4.12 PV curve for the case with P control and MRAC

Fig. 4.13 is comparison between the P control with/without MRAC. We observe that HB is pushed to higher load and therefore the adaptive control is able to increase the system's loadability.

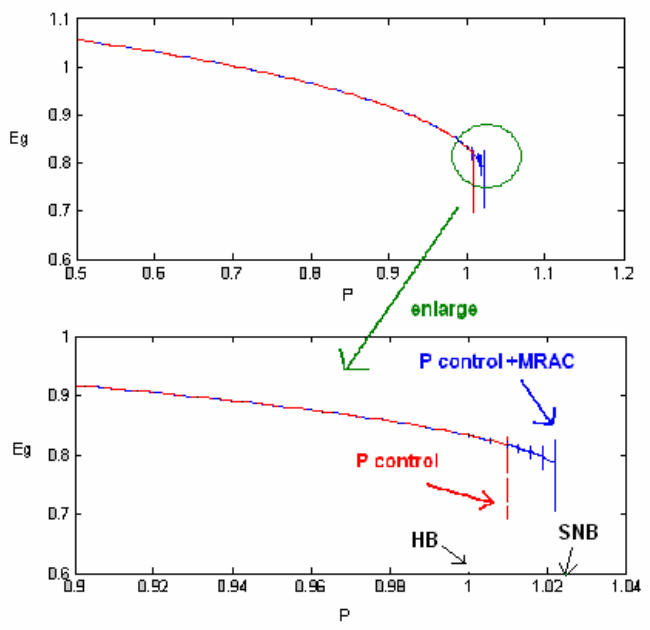

Fig. 4.13 Comparison of MRAC for the case with P control

4.2.3 Third-order example (the system with PI control)

Consider the 2-bus power system with PI controller as below,

$$\dot{E}' = \frac{1}{T_{d0}'}\left[-\frac{x+x_d}{x'}E' + \frac{x_d - x_d'}{x'}\frac{E^2 + x'Q}{E'} + E_{fd}\right] \tag{4.32}$$

$$\dot{E}_{fd} = \frac{1}{T}\left[-(E_{fd} - E_{fd0} - \Delta E_{fd0}) - K(E_g - E_r)\right] \tag{4.33}$$

$$\dot{\Delta E}_{fd} = \gamma(E_r - E_g) \tag{4.34}$$

$$0 = E'^2 E^2 - (x'P)^2 - (x'Q + E^2)^2 \tag{4.35}$$

$T_{d0}' = 5,\ T = 1.5,\ E_{fd0} = 1.6,\ x_d = 1.2,\ x_d' = 0.2,$
$x = 0.1,\ x' = x + x_d',\ Q = 0.5P,\ E_r = 1.0, K = 3.2,\ \gamma = 0.1$

<**Step 1**> Find Equilibrium value of E_g

From (4.34), we know $E_{ge} = E_r = 1$, no matter the load $\{P, Q\}$ change. Therefore, we do not need equilibrium tracking mechanism.

<**Step 2**> Apply MRAC

We choose model reference which relative degree is two as (4.36)

$$W_m(s) = \frac{1}{s^2 + s + 1} \tag{4.36}$$

Therefore, the desired trajectory y_m is generated by

$$\begin{aligned} \dot{w}_0 &= \begin{bmatrix} -1 & -1 \\ 1 & 0 \end{bmatrix} w_0 + \begin{bmatrix} 1 \\ 0 \end{bmatrix} r \\ y_m &= \begin{bmatrix} 0 & 1 \end{bmatrix} w_0 \end{aligned} \tag{4.37}$$

where r is the reference input of reference model.

Let feedback control law Δu_p as (4.38)

$$u_p = \dot{\theta}^T \phi + \theta^T w \tag{4.38}$$

Where w is generated by

$$\dot{w}_1 = F w_1 + g \Delta u_p \tag{4.39}$$

$$\dot{w}_2 = F w_2 + g(E_g - \hat{E}_{ge}) \tag{4.40}$$

And ϕ is generated by

$$\dot{\phi} = -p_0\phi + w \tag{4.41}$$

where $w = [w_1^T, w_2^T, (E_g - \overset{\Lambda}{E}_{ge}), r]^T$

Choose $F = \begin{bmatrix} -2 & -1 \\ 1 & 0 \end{bmatrix}$, $g = \begin{bmatrix} 1 \\ 0 \end{bmatrix}$, $p_o = 1.$

The controller parameter θ is directly generated by the adaptive law

$$\dot{\theta} = \Gamma e_1 \phi \,\mathrm{sgn}(k_p / k_m) \tag{4.42}$$

where $\mathrm{sgn}(k_p / k_m) = 1$

Choose $\Gamma = 1000$ and $e_1 = (E_g - \overset{\Lambda}{E}_{ge}) - y_m$

By equations (4.2.32)-(4.2.42), we have an original DAE system with an auxiliary adaptive control. The Fig. 4.14 shows block diagram for the original DAE system with MRAC.

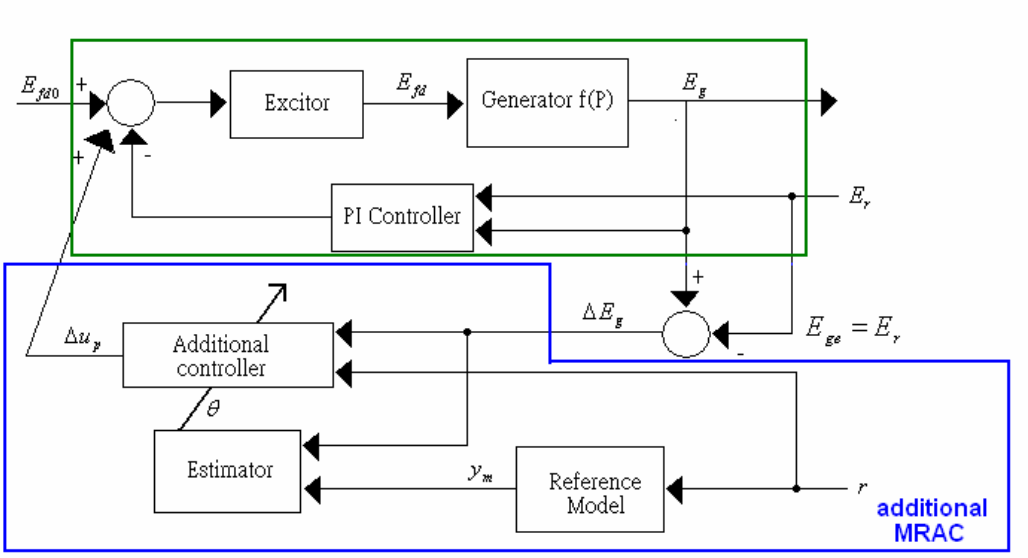

Fig. 4.14 Block diagram of the two bus system with PI control and MRAC

(1) Simulation results

Without MRAC

As load gradually increasing and over HB, we observe that trajectories oscillate and diverge as the Fig. 4.15 From the figure, we also see that generator bus voltage is equal to one no matter power load change.

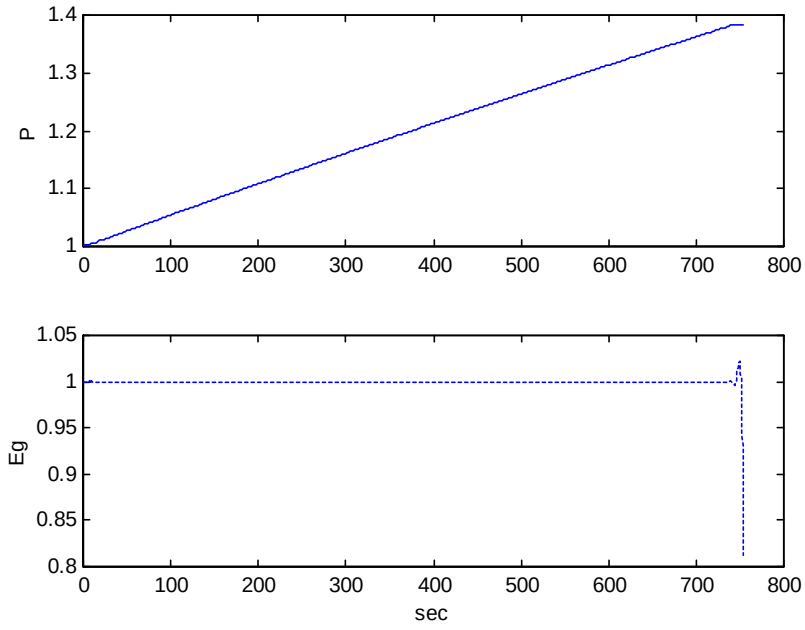

Fig. 4.15 Time response of generator bus voltage as load increases for the case with PI control without MRAC

Accordingly, we draw the PV curve as the Fig. 4.16.

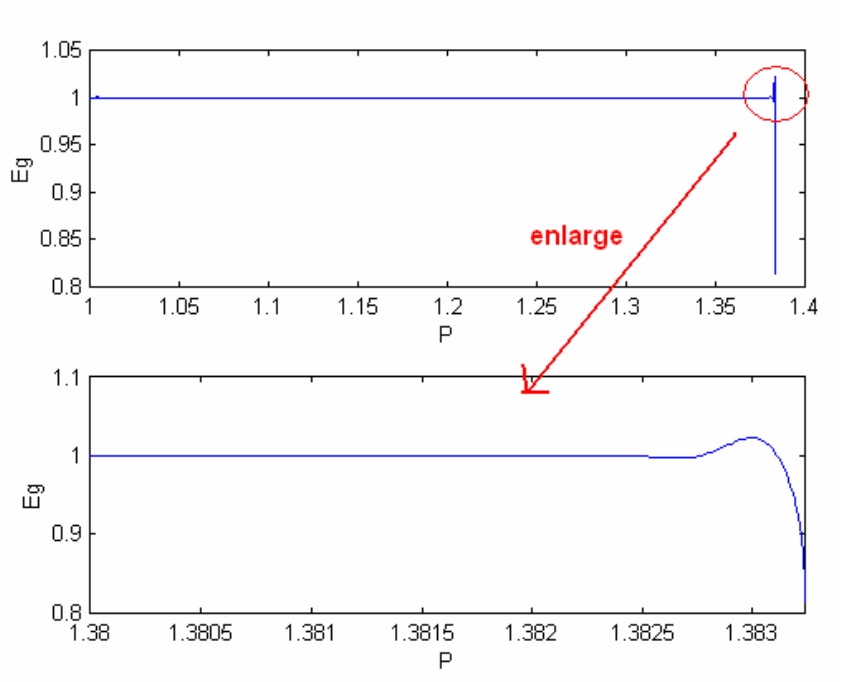

Fig. 4.16 PV curve for the system with PI control without MRAC

With MRAC

Similarly, as power load gradually increasing, we observe its time response for generator bus voltage (Fig. 4.17) and the feedback signal and the estimated control parameter (Fig. 4.18).

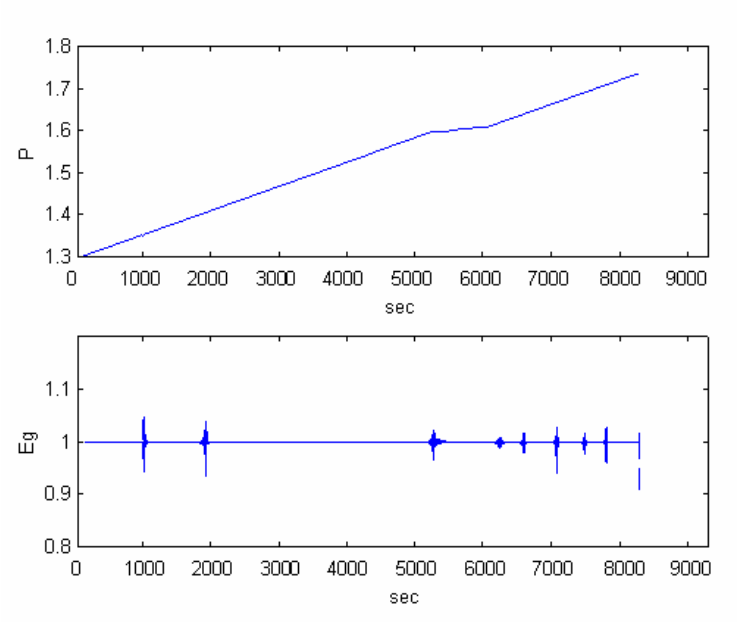

Fig. 4.17 Time response for generator bus voltage as load increases for the case with PI control and MRAC

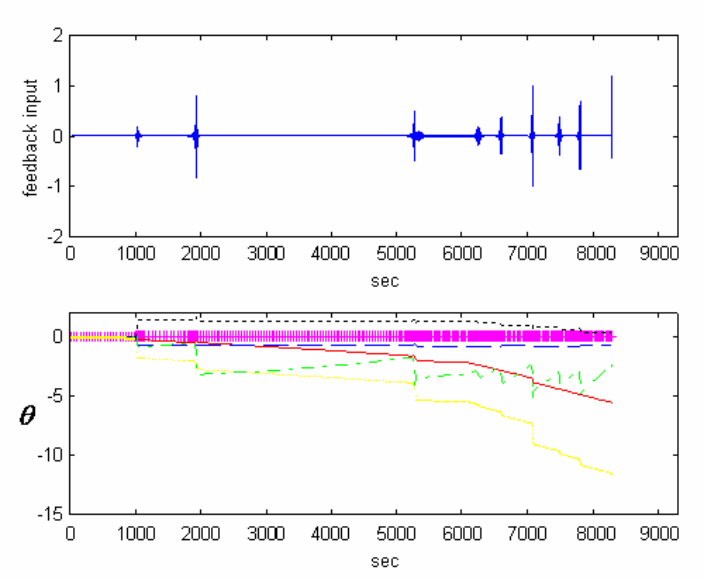

Fig. 4.18 Feedback signal and estimated control parameters for PI control with MRAC

And then we draw its corresponding PV curve in Fig. 4.19.

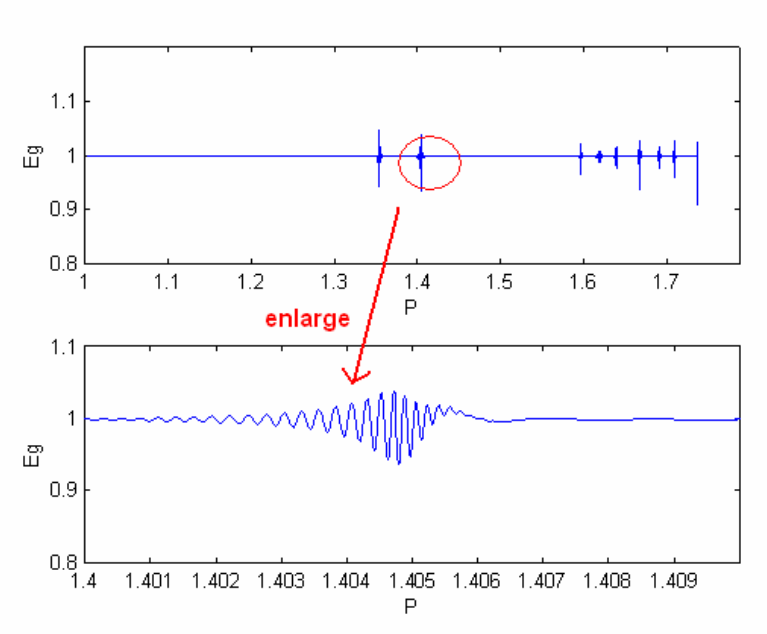

Fig. 4.19 PV curve for the system with PI control and MRAC

Fig. 4.20 shows the comparison between the PI control with/without MRAC. Similarly, our additional MRAC pushes HB to higher load and therefore increasing the system's loadability.

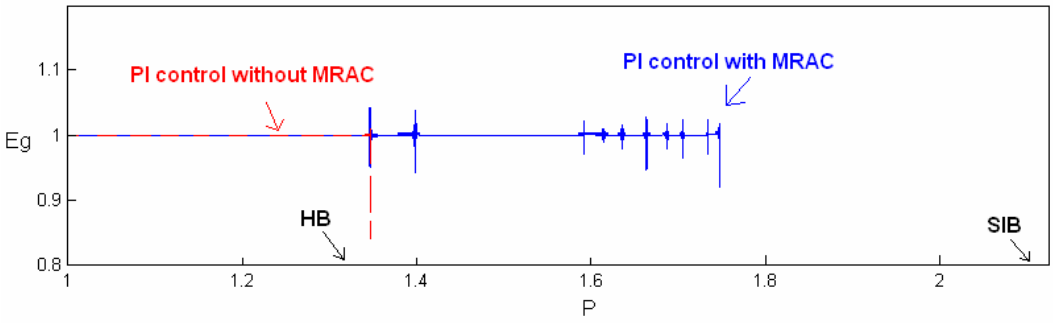

Fig. 4.20 Comparison of MRAC for the case with PI control

4.2.4 Comparison between the system with/without P/PI control and with/without MRAC

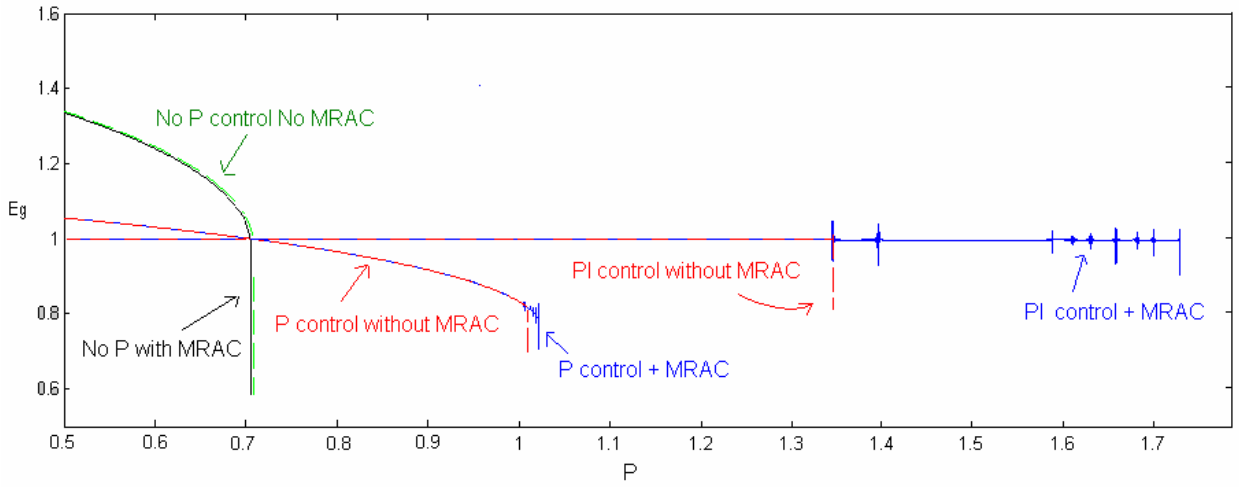

Fig. 4.21 Comparison of PV curve for different controller

Again, we should emphasize that our control design is to stabilize the equilibrium along the original PV curve but not change the PV curve. Thus, we still need the PI or P control to get better shape of PV curve and regulation. See Fig. 4.21, if without PI/P control, voltage will drop too dramatically when power load increase whether the system with MRAC or not. Otherwise, for the case of the system without P/PI control, our MRAC fail to increase the system's loadability.

4.3 Limitation and Choice of Coefficients

(1) For the 'real' linear system, the MRAC and APPC schemes we used are suitable for any initial condition. However, for nonlinear system, Since we designed the adaptive based on approximation around equilibrium points, the stability properties is only hold for a small enough neighborhood of the equilibrium point.

(2) Usually, if we set reference input $r \equiv 0$, the estimate parameters do not converge to its true value. It only guarantees all bounded signals and stability. If r,however, has sufficient frequency components, the estimate parameters will converge to its true value (just like the reference model). And the converge time depends on the amplitude of r. Smaller amplitude of r makes converge time longer.

(3) Larger Γ would make trajectories converge faster. See Fig. 4.22 and Fig. 4.23. When $\Gamma = 500$ ($\gamma = 500$), the trajectories converge before singularity. Besides, we observe that for the same system, the higher load, the faster trajectories diverge. Thus, we need the larger Γ for the higher load.

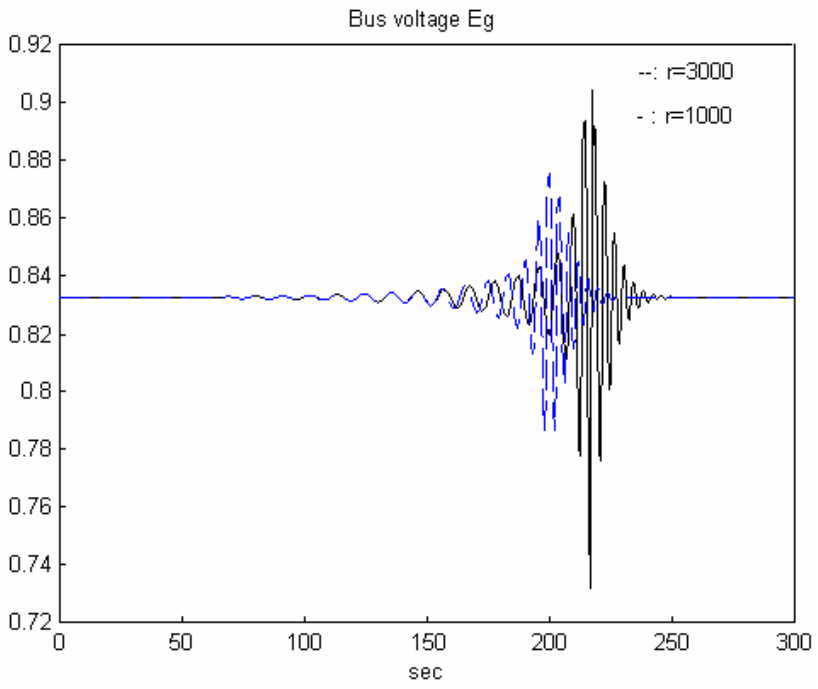

Fig. 4.22 Time response of bus voltage for $\Gamma = 3000$ and $\Gamma = 1000$

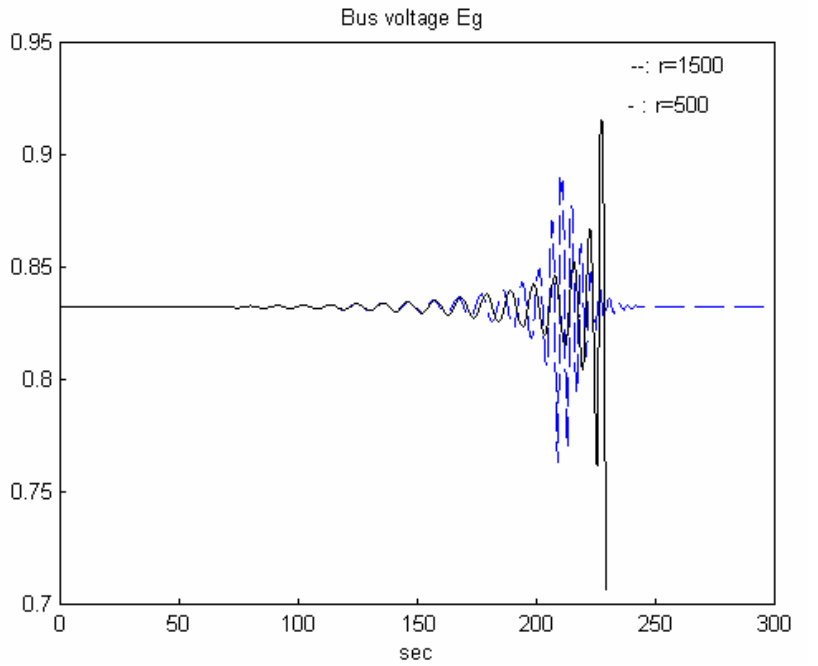

Fig. 23 Time response of bus voltage for $\Gamma = 1500$ and $\Gamma = 500$

4.4 Summary

Our exciter control combines the original PI/P controller with an additional controller which is used to stabilize all existing equilibrium along the original PV curve. If the power load is lower than HB (the equilibrium is stable), since the trajectories would be close to the equilibrium manifold ($|\Delta E_g| < \varepsilon$), our additional controller will not be activated. But if power load increased to over HB (the equilibrium becomes unstable), since the trajectories will diverge from the equilibrium manifold ($|\Delta E_g| > \varepsilon$), our controller will be activated and adjusting the controller parameters until the system become stable ($|\Delta E_g| < \varepsilon$ again). Actually, we can consider the controller will be activated whenever $|\Delta E_g| > \varepsilon$.

By our approach, the system can enhance the robustness as well as increase the system's loadability.

Otherwise, the adaptive schemes and control law we use in the thesis are based on a plant model that is free of disturbance and unmodeled dynamics which would be especially due to nonlinearity in our application. The discrepancies between the linearized model and the actually plant may lead to instability [17]. These error effects, however, can be improved by some modification such as leakage, dead zone, projection or σ–modification [10][18][19] which are known as robust adaptive control.

CHAPTER V
CONCLUSION

This thesis addresses the dynamic modeling issues of power system application. We introduce the systematic description and dynamic voltage stability in power systems. Mathematically, power systems are commonly modeled by differential-algebraic equations (DAE). The differential equations describe the slow dynamics such as generator dynamics, excitation control system. The algebraic equations are corresponding to the power flow equations, which are fast mode compared with the slow ones of generation parts.

The objective of the thesis is design an adaptive control to stabilize at the equilibrium point when it exists for a general parameter-dependent DAE system. In the thesis, we focus on the excitation voltage control of power system and desire to design an auxiliary control to improve oscillatory instability, it is related to Hoph Bifurcation, and therefore increase the system's loadability.

To achieve our goal, our approaches are to improve the structure stability of the DAE system i.e., we stabilize all the existing equilibrium whenever stable or unstable. In the practical points of view, the equilibrium exists if power flow equation has solutions. Once power flow equation doesn't exist, it is so-called voltage collapse [3], one should reset the operation condition or change parameters to shape a new PV curve. In the thesis, however, we just consider the condition when power flow solution exists and stabilize all the equilibrium along the original PV curve.

To realize the objective, we propose MRAC and APPC schemes to build a control which can sense the system parameter variation to adjust control parameters and lead the system to be stable. In fact, from the time response simulation, oscillatory instability can be inferred from diverged oscillatory trajectories. Our controls are just able to inspect the diverged trajectories and force trajectories become converge by dynamically changing its control parameters.

Now, let us summarize our conclusion:

- The overall control input is $u = u_{ss} + \Delta u_p$ where u_{ss} is feedforward control which can be referred to as set-point and Δu_p is our auxiliary feedback control Δu_p which is implemented by the adaptive control schemes. Then, the original DAE system with our control can be describe by

$$\begin{aligned} \dot{x} &= f(x, y, p, u) \\ 0 &= g(x, y, p, u) \end{aligned} \tag{5.1}$$

- For the DAE system (5.1), we track the equilibrium value x_{ei} for its corresponding p_i satisfying,

$$\begin{aligned} 0 &= f(x_{ei}, y_{ei}, p_i, u_{ss}) \\ 0 &= g(x_{ei}, y_{ei}, p_i, u_{ss}) \end{aligned} \tag{5.2}$$

Since x_{ei} is not available, instead of using the true value of x_{ei}, we use an estimator $\hat{x}_{ei}$ implemented by (5.3)

$$\dot{\hat{x}}_{ei} = \beta(x - \hat{x}_{ei}) \tag{5.3}$$

With $\beta > 0$.

- The dynamic properties around a enough small neighborhood of x_{ei} is as below

$$\Delta \dot{x} = A_i \Delta x + B_i \Delta u_p \tag{5.4}$$

Thus, by MRAC or APPC, we have a direct adaptive control Δu_p

$$\Delta u_p = C(\theta_c, \Delta x) \tag{5.5}$$

$$\dot{\theta}_c = h(\theta_c, \Delta x) \tag{5.6}$$

Or an indirect adaptive control

$$\Delta u_p = C(\theta_c, \Delta x) \tag{5.7}$$

$$\theta_c = F(\theta_p) \tag{5.8}$$

$$\dot{\theta}_p = h(\theta_p, \Delta x) \tag{5.9}$$

Then, we resolve the problem of the equilibrium stability of the closed-loop

$$\Delta \dot{x} = A_i \Delta x + B_i \Delta u_p(\theta_c, \Delta x)$$

By the approaches, we can improve oscillatory instability and strengthen the power

system’s ability to accommodate parameter uncertainty. The digital excitation can easily implement such an adaptive control without increasing cost.

REFERENCES

[1] C. Vournas, *Voltage Stability of Electric Power Systems.* Boston: Kluwer Academic Publishers, 1998.

[2] T. V. Cutsem, "Voltage instability: Phenomena, countermeasures, and analysis methods," *Proceedings of the IEEE*, vol. 88, no. 2, pp. 208-227, Feb. 2000.

[3] P. Kundur, *Power System Stability and Control.* New York: McGraw-Hill, 1994.

[4] N. N. Bengiamin, W.C. Chan, "Variable structure control of electric power generation," *IEEE Trans. on Power Apparatus and Systems*, vol. PAS-101, no. 2, pp. 376-380, Feb. 1981.

[5] M.E. Aggoune, F. Boudjemaa, A. Bensenouci, A. Hellal, S.V. Vadari and M.R. Elmesai, "Design of variable structure voltage regulator using pole assignment technique," *IEEE Trans. on Automatic Control*, vol. 39, no. 10, pp. 2106-2110, Oct.1994.

[6] L. Gao, L. Chen, Y. Fan and H. Ma, "A nonlinear control design for power systems," *Automatica*, vol.28, no. 5, pp 975-979 Sep. 1992.

[7] Y. Wang , D. J. Hill and R. H. Middleton, "Transient stability enhancement and voltage regulation of power systems," *IEEE Trans. on Power Systems*, vol.8 , no. 2, pp. 620-627, May 1993.

[8] Y. Wang , D. J. Hill, L. Gao and R. H. Middleton, "Transient stabilization of power systems with an adaptive control law," *Automatica*, vol.30, no. 9, pp. 1409-1413, Sep. 1994.

[9] H. K. Khalil, *Nonlinear Systems*, Englewood Cliffs, NJ: Prentice Hall, 2002.

[10] P. Ioannou and J. Sun, *Robust Adaptive Control*, Englewood Cliffs, NJ: Prentice Hall, 1996.

[11] M. Shoji, *The Dynamics of Digital Excitation*, Boston: Kluwer Academic Publishers, 1998.

[12] A. B. Bergen, V. Vittal, *Power System Analysis*, Englewood Cliffs, NJ: Prentice Hall 1999.

[13] J. J. Grainger, *Power System Analysis*, New York: McGraw-Hill, 1994.

[14] V. Venkatasubramanian, H. Schaettler and J. Zaborazky, "Local bifurcation feasibility regions in differential –algebraic systems," *IEEE Trans. on Automatic Control*, vol. 40, no.12, pp. 1992-2031, Dec.1995.

[15] V. Venkatasubramanian, H. Schaettler and J. Zaborazky, "Voltage dynamics: study of a generator with voltage control, transmission, and matched MW load," *IEEE Trans. on Automatic Control*, vol 31, no. 11, pp.3045-3056, Nov.1992.

[16] G. M. Huang, L. Zhao, and X. Song, "A new bifurcation analysis for power system dynamic voltage studies," in *Proc. IEEE Power Engineering Society Winter Meeting*, 2002, vol.2, pp.882-887, Jan. 2002.

[17] C. E. Rohrs, L. Valavani, M. Athans, and G. Stein "Robustness of continuous-time adaptive control algorithm in the presence of unmodeled dynamics," *IEEE Trans. on Automatic Control*, vol.30, no.9, pp.881-889, Sep. 1985.

[18] G. Tao, and P.A. Ioannou, "Robust stability and performance improvement of multivariable Plants," *Int. J. of Control*, vol. 50, no.5, pp.1835-1855, May 1989.

[19] K. S. Tsakalis, “Robustness of model reference adaptive controllers: an input-output approach,” *IEEE Trans. on Automatic Control*, vol. 37, no.5, pp.556-565, May 1992.

VITA

Name: Pei-Chen Chiu

Address: No. 39, Aly. 38, Ln 57, HEPING E ST. SEC.1 YUANLIN J, Chanhua 510, Taiwan.

Email address: master_ece87@yahoo.com.tw

Education: B.S., Electrical and Control Engineering, National Chiao Tung University, 2002

M.S., Electrical Engineering, Texas A&M University, 2006